Andreev reflection at half-metal/superconductor interfaces with nonuniform magnetization

Joern N. Kupferschmidt[1,2] and Piet W. Brouwer[2]

[1]*Laboratory of Atomic and Solid State Physics, Cornell University, Ithaca, New York 14853-2501, USA*

[2]*Dahlem Center for Complex Quantum Systems and Institut für theoretische Physik, Freie Universität Berlin, Arnimallee 14, D-14195 Berlin, Germany*

(Received 16 September 2010; revised manuscript received 23 November 2010; published 20 January 2011)

Andreev reflection at the interface between a half-metallic ferromagnet and a spin-singlet superconductor is possible only if it is accompanied by a spin flip. Here we calculate the Andreev reflection amplitudes for the case where the spin flip originates from a spatially nonuniform magnetization direction in the half-metal. We calculate both the microscopic Andreev reflection amplitude for a single reflection event and an effective Andreev reflection amplitude describing the effect of multiple Andreev reflections in a ballistic thin film geometry. It is shown that the angle and energy dependence of the Andreev reflection amplitude strongly depends on the orientation of the gradient of the magnetization with respect to the interface. We calculate the resulting effects on the subgap conductance as well as Josephson current for a few exemplary cases. Establishing a connection between the scattering approach employed here and earlier work that employs the quasiclassical formalism, we connect the symmetry properties of the Andreev reflection amplitudes to the symmetry properties of the anomalous Green function in the half-metal.

DOI: 10.1103/PhysRevB.83.014512 PACS number(s): 74.45.+c, 74.78.Na, 75.70.Cn

I. INTRODUCTION

Superconductors extend their order into adjacent normal metals via the mechanism of Andreev reflection:[1] An electron incident on the superconductor–normal-metal interface is phase-coherently reflected as a hole, and vice versa.[2] Half-metallic ferromagnets (half-metals) are normal metals that support quasiparticle excitations of only one spin orientation. If superconducting correlations are to extend from a spin-singlet superconductor into a half-metallic ferromagnet, the azimuthal spin-rotation symmetry around the magnetization axis needs to be broken near the superconductor–half-metal interface, so that electrons can be Andreev reflected into holes in the same spin band.

In standard ferromagnets (which have majority as well as minority carriers), such a combination of spin-flip and Andreev reflection was shown theoretically[3–6] and experimentally [7–10] to lead to a superconductor proximity effect with a range comparable to that in normal metals. In the literature, magnetic domain walls,[3–5,11–14] helical structures intrinsic to the ferromagnetic material,[14–17] artificially structured multilayers with noncollinear magnetization directions in different layers,[18–22] and a precessing magnetization direction[23] were addressed as possible microscopic origins of the broken spin-rotation symmetry. Although the possibility of spin-flip Andreev reflection (with similar origins) also exists for half-metal–superconductor interfaces,[20,24–29] and a sizable Josephson current has been observed in junctions involving a half-metallic ferromagnet,[30,31] the Andreev reflection mechanism at half-metal–superconductor interfaces was found to be more delicate than in the case of standard ferromagnets.[29]

The underlying reason for the differences between a ferromagnet–superconductor (FS) interface and a half-metal–superconductor (HS) interface is that, if no orbital symmetries are broken, the latter admits a description in terms of an effective 2×2 scattering matrix, whereas the former requires at least a 4×4 scattering matrix, to account for the spin degree of freedom. Mathematical constraints on 2×2 matrices following from current conservation and particle-hole symmetry then force the Andreev reflection amplitude $r_{\rm he}(\varepsilon)$ of an HS junction to be generically zero at the Fermi level $\varepsilon = 0$, whereas there is no such strong restriction on the Andreev reflection amplitudes for an FS junction. As shown in Ref. 29, the fact that $r_{\rm he}(0) = 0$ for an HS junction has little consequences for the strength of the proximity effect at distances below the superconducting coherence length $\xi_{\rm S}$, but leads to a suppression of the proximity effect at larger distances in comparison to a normal-metal–superconductor (NS) junction.[29] For example, the zero-temperature critical current in a ballistic SHS junction of length $L \gg \xi_{\rm S}$ is a factor $\sim (L/\xi_{\rm S})^2$ smaller than in an otherwise comparable SFS junction.[29] (The experiments of Refs. 30,31, which observe a sizable Josephson effect in SHS junctions, have $L \sim \xi_{\rm S}$, so that they need not be affected by this effect.)

If orbital symmetries are broken, the mathematical constraints leading to the condition $r_{\rm he}(\varepsilon) = 0$ at $\varepsilon = 0$ are no longer operative. Examples of broken orbital symmetries that allow for a finite Andreev reflection amplitude $r_{\rm he}(\varepsilon)$ at $\varepsilon = 0$ are a magnetization gradient parallel to the interface, spin-orbit coupling in the superconductor, unconventional symmetry of the superconducting order parameter—which all break inversion symmetry with respect to the interface normal—or impurity scattering. Andreev reflection in the presence of a magnetization gradient parallel to the interface, which is relevant for a domain wall in the half-metal, was previously considered by us in Ref. 32 in the limiting case of a half-metal with infinite wave function decay rate $\kappa_\downarrow$ of the minority carriers. This situation will be analyzed in more detail here. We lift simplifying assumptions of Ref. 32, and compare the generalized result to the case when the magnetization varies perpendicular to the interface, where no orbital symmetry is broken. Andreev reflection at interfaces between a half-metal and a superconductor with unconventional pairing was considered by Linder *et al.* in Ref. 33. The other two

scenarios for breaking orbital symmetries will be analyzed elsewhere.[34,35]

The scenario of a magnetization gradient parallel to the HS interface is particularly relevant for a lateral superconductor–half-metal contact, for which the superconducting contact is deposited on top of a half-metallic film. The experiments of Refs. 30,31 were performed in such a lateral geometry. A lateral contact, with a domain wall in the half-metal under the contact area, is shown schematically in Fig. 1. For a phase-coherent lateral contact, it is convenient to define an "effective" Andreev reflection amplitude $r_{\rm he}^{\rm eff}$ that represents the effect of multiple Andreev reflections at the HS interface for a quasiparticle moving in the thin half-metallic film, incident on a domain wall (or any other region with nonuniform magnetization) from a region with uniform magnetization, see Fig. 1c. (The standard definition of the Andreev reflection amplitude $r_{\rm he}$ is for single incidence of a quasiparticle onto the superconductor interface. This is the situation shown in Fig. 1b.) Because one is interested in currents flowing parallel to the interface in a lateral contact (see Fig. 1c), it is the effective amplitude $r_{\rm he}^{\rm eff}$, not $r_{\rm he}$, which occurs in a calculation of, e.g., the subgap conductance or the Josephson current.[32]

In this article, we calculate both the microscopic Andreev reflection amplitudes $r_{\rm he}$ and the effective amplitude $r_{\rm he}^{\rm eff}$. We consider an HS interface with a low normal-state transmission probability, caused by the presence of a tunnel barrier or by the mismatch of Fermi velocities on both sides of the junction. We do not consider the effect of impurity scattering.

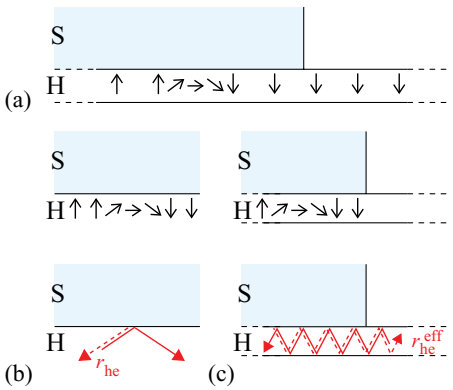

FIG. 1. (Color online) (a) Lateral contact between a thin half-metallic film (H) and a superconductor (S). Andreev reflection at the HS interface is possible at those interface positions where the magnetization direction (indicated by thin black arrows) is not uniform, such as a domain wall. The situation shown in the figure is generic, since domain walls at the HS interface are bound to occur if the HS contact is larger than the domain size in the half-metallic film. In this geometry, there are two possible ways to define the Andreev reflection amplitude: The amplitude $r_{\rm he}$ for a single Andreev reflection (filled red arrows), appropriate for the interface between a semi-infinite half-metal and a superconductor (b), and the effective amplitude $r_{\rm he}^{\rm eff}$ representing the combined effect of multiple Andreev reflections in the same region of nonuniform magnetization for quasiparticles moving in the half-metallic film (c). In (b) and (c), the black arrows in the top panel show the spatial variation of the magnetization direction, whereas the filled red arrows in the bottom panel show an example of a trajectory for an incoming electron (solid) and an Andreev reflected hole (dashed).

For the calculation of $r_{\rm he}$ this is not a serious shortcoming as Andreev reflection is local, and only impurities in the immediate vicinity of the interface would play a role (up to distances of the order of a Fermi wavelength). For the effective Andreev reflection amplitude $r_{\rm he}^{\rm eff}$ in the thin-film geometry, the omission of impurity scattering limits the applicability of our results to situations in which the mean free path is larger than the domain wall size $l_{\rm d}$ (or even the contact size, if the region of nonuniform magnetization extends along the entire lateral contact). In addition to the scenario of a magnetization gradient parallel to the HS interface, we also consider the case that the magnetization gradient is perpendicular to the HS surface as is relevant, e.g., if the half-metal has different boundary and bulk anisotropies.

The calculation of the microscopic, single-reflection amplitude $r_{\rm he}$ will be presented first. Hereto, we first review the restrictions of symmetry on Andreev reflection at a HS interface in Sec. II. We then introduce the Hamiltonian and the wave functions for the case of a uniform magnetization in Sec. III. The calculation of the Andreev reflection amplitudes in the presence of a nonuniform magnetization then takes place in Sec. IV. The calculation of the effective Andreev reflection amplitude $r_{\rm he}^{\rm eff}$ for a superconductor placed on top of a thin half-metallic film is then presented in Sec. V. In Secs. IV and V we also discuss applications of our results to the subgap conductance of an HS junction and the Josephson current in an SHS junction. Finally, in Sec. VI, we discuss the relation of the scattering approach used in this article and the Green function approach used in most of the literature. In particular, we consider the anomalous Green function and its frequency dependence. We conclude in Sec. VII. The Appendix contains certain details of the calculations not presented in the main text.

II. CONSTRAINTS IMPOSED BY UNITARITY AND PARTICLE-HOLE DEGENERACY

Although the considerations of this section are completely general, for definiteness we choose coordinates such that the half-metal–superconductor interface is the plane $z = 0$. In this section and in the following two sections, the half-metal occupies the half-space $z < 0$, and the superconductor, which is taken to be of s-wave, spin-singlet type, occupies the half-space $z > 0$. This setup is shown schematically in Fig. 2.

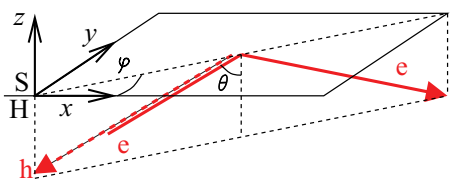

FIG. 2. (Color online) Illustration of the scattering setup. Coordinates are chosen, such that the half-metal–superconductor interface is the plane $z = 0$. Electron-like quasiparticles incident on the HS interface are either reflected as an electron (normal reflection), or as a hole (Andreev reflection). At a translationally invariant interface, the projection $\mathbf{k}_\parallel$ of the wave vector on the interface is conserved upon reflection.

Quasiparticles in the half-metal are labeled by their wave vector $\mathbf{k}_\parallel = k_x\mathbf{e}_x + k_y\mathbf{e}_y$ parallel to the HS interface ($\mathbf{e}_x$ and $\mathbf{e}_y$ are unit vectors in the x and y directions, respectively) and by their excitation energy ε. We assume periodic boundary conditions in the x and y directions, so that the wave vectors $\mathbf{k}_\parallel$ are discrete.

At excitation energies ε below the superconducting gap Δ, quasiparticles incident on the half-metal–superconductor interface from the half-metallic side will be reflected back into the half-metal. This reflection can be either normal reflection or Andreev reflection, for which electron-like quasiparticles are reflected as holes and vice versa. The reflection process is described by a scattering matrix $\mathcal{S}(\mathbf{k}'_\parallel,\mathbf{k}_\parallel;\varepsilon)$, which takes the form

$$\mathcal{S}(\mathbf{k}'_\parallel,\mathbf{k}_\parallel;\varepsilon) = \begin{pmatrix} r_{\rm ee}(\mathbf{k}'_\parallel,\mathbf{k}_\parallel;\varepsilon) & r_{\rm eh}(\mathbf{k}'_\parallel,\mathbf{k}_\parallel;\varepsilon) \\ r_{\rm he}(\mathbf{k}'_\parallel,\mathbf{k}_\parallel;\varepsilon) & r_{\rm hh}(\mathbf{k}'_\parallel,\mathbf{k}_\parallel;\varepsilon) \end{pmatrix}, \tag{1}$$

where the subscripts e and h refer to electron-like and hole-like states. The scattering amplitudes $r_{\rm eh}$ and $r_{\rm he}$ describe Andreev reflection processes.

The scattering matrix $\mathcal{S}(\mathbf{k}'_\parallel,\mathbf{k}_\parallel;\varepsilon)$ satisfies two constraints: Unitarity and particle-hole symmetry. The latter condition reads

$$\mathcal{S}(\mathbf{k}'_\parallel,\mathbf{k}_\parallel;\varepsilon) = \begin{pmatrix} 0 & 1 \\ 1 & 0 \end{pmatrix} \mathcal{S}(-\mathbf{k}'_\parallel,-\mathbf{k}_\parallel;-\varepsilon)^* \begin{pmatrix} 0 & 1 \\ 1 & 0 \end{pmatrix}. \tag{2}$$

The combination of unitarity and particle-hole degeneracy severely restricts the form of the scattering matrix if there is translation invariance along the interface, which implies

$$\mathcal{S}(\mathbf{k}'_\parallel,\mathbf{k}_\parallel;\varepsilon) = \mathcal{S}(\mathbf{k}_\parallel;\varepsilon)\,\delta_{\mathbf{k}'_\parallel,\mathbf{k}_\parallel}. \tag{3}$$

Combination of Eqs. (2) and (3) gives

$$\begin{aligned} r_{\rm ee}(\mathbf{k}_\parallel,\varepsilon) &= r_{\rm hh}(-\mathbf{k}_\parallel,-\varepsilon)^*, \\ r_{\rm eh}(\mathbf{k}_\parallel,\varepsilon) &= r_{\rm he}(-\mathbf{k}_\parallel,-\varepsilon)^*. \end{aligned} \tag{4}$$

If the scattering problem is also invariant for a π rotation around the interface normal, so that

$$\mathcal{S}(\mathbf{k}'_\parallel,\mathbf{k}_\parallel;\varepsilon) = \mathcal{S}(-\mathbf{k}'_\parallel,-\mathbf{k}_\parallel;\varepsilon), \tag{5}$$

one finds, upon combining all symmetry properties,

$$r_{\rm ee}(\mathbf{k}_\parallel;0) r_{\rm eh}(\mathbf{k}_\parallel;0) = 0 \tag{6}$$

for the scattering matrix at the Fermi level $\varepsilon = 0$. Since $r_{\rm ee} \neq 0$, except for a special choice of parameters, this implies that generically one must have[29]

$$r_{\rm eh}(\mathbf{k}_\parallel;0) = 0. \tag{7}$$

These very general considerations pose a severe restriction on the magnitude and the spatial extension of the proximity effect in half-metals that is absent in ferromagnet–superconductor junctions with otherwise comparable characteristics. A nonzero Andreev reflection amplitude for a half-metal–superconductor junction can be obtained only by fine-tuning device parameters such that the normal reflection amplitude becomes zero, or by invoking processes that break the symmetries leading to Eq. (7). The former scenario was discussed in Ref. 29 and will not be addressed here. Examples of symmetry-breaking processes that result in a nonzero Andreev reflection amplitude are: lifting of particle-hole degeneracy by a finite excitation energy ε,[29,36] breaking of the rotation symmetry around the interface normal,[32] breaking of the translation symmetry along the interface, or the breaking of phase coherence.[37] A domain wall for which the magnetization direction varies in a direction parallel to the interface is an example of a perturbation that breaks the rotation symmetry.[32] However, a thin interface layer of different magnetic orientation than the interior of the half-metal (which is a model of a "spin-active interface"[24–27,38]) does not lift the constraints leading to Eq. (7).[29,36] The role of variations in the magnetization direction will be considered in more detail in Sec. IV below.

A finite excitation energy ε lifts the particle-hole degeneracy, and the Andreev reflection amplitude $r_{\rm eh}$ becomes nonzero. If no other symmetries are broken, the order of magnitude of the Andreev reflection amplitudes at finite ε can be estimated as

$$|r_{\rm eh}(\varepsilon)| \sim \frac{|\varepsilon|}{\min(\Delta/\tau, E_\xi)} |r_{\rm eh,\,FS}|, \tag{8}$$

where E_ξ is the Thouless energy of the interface layer where the singlet-triplet conversion takes place, τ is the transparency of the superconductor interface, Δ the superconducting gap, and $r_{\rm eh,\,FS}$ the Andreev reflection amplitude of a ferromagnet–superconductor amplitude of otherwise comparable characteristics. The first energy scale in the denominator comes about because electrons and holes scattering off a normal-metal–superconductor interface of transparency τ at finite excitation energy ε experience an additional phase difference $\sim \pm\varepsilon\tau/\Delta$, which lifts the electron-hole degeneracy.[39] The second energy scale in the denominator appears from phase differences acquired in the interface layer. The typical thickness of this interface layer is of the order of minority decay length ξ, which implies that E_ξ is of the order of the Fermi energy. For tunneling interfaces one always has $|r_{\rm eh}(\varepsilon)| \ll |r_{\rm eh,\,FS}|$ and we conclude that the breaking of electron hole symmetry by finite excitation energies is not an efficient route toward sizable Andreev reflection in that case. The suppression of Andreev reflection in half-metal–superconductor junctions (as compared to ferromagnet–superconductor junctions) is absent only for transparent interfaces and excitation energies of order Δ.

The ε-dependence of $r_{\rm eh}$ not only determines the conductance through the half-metal–superconductor interface at finite bias,[29,36] it also sets the scale for the Josephson effect in a superconductor-half-metal–superconductor junction.[40,41] If the Thouless energy E_L of a Josephson junction of length L is large in comparison to Δ ("short junction limit"), the Josephson current I is carried by quasiparticle states with energies up to Δ. In this limit, the symmetry considerations that suppressed Andreev reflection at $\varepsilon = 0$ do not affect the order of magnitude of I, and one concludes that otherwise comparable superconductor-half-metal–superconductor and superconductor–ferromagnet–superconductor junctions have comparable Josephson currents.[29] If, however, $E_L \ll \Delta$ ("long junction limit"), only quasiparticle states with energy below E_L contribute to I, so that I is significantly suppressed compared to the Josephson current in comparable superconductor–ferromagnet–superconductor junctions.

In the remainder of this article, we present explicit model calculations of the Andreev reflection amplitudes for the case that singlet-triplet conversion is mediated by a spatially nonuniform magnetization in the half-metal, as it appears, e.g., in a domain wall.

III. HAMILTONIAN AND SCATTERING STATES

A. Bogoliubov–de Gennes Hamiltonian

Quasiparticle excitations near the HS interface are described by the Bogoliubov–de Gennes equation[42]

$$\mathcal{H}\Psi(\mathbf{r}) = \varepsilon\Psi(\mathbf{r}), \quad \mathcal{H} = \begin{pmatrix} \hat{H} & i\Delta e^{i\phi}\sigma_2 \\ -i\Delta e^{-i\phi}\sigma_2 & -\hat{H}^* \end{pmatrix}, \tag{9}$$

where the four-component spinor

$$\Psi(\mathbf{r}) = [u_\uparrow(\mathbf{r}), u_\downarrow(\mathbf{r}), v_\uparrow(\mathbf{r}), v_\downarrow(\mathbf{r})]^{\mathrm{T}} \tag{10}$$

consists of wave functions $u_\sigma(\mathbf{r})$ for the electron and $v_\sigma(\mathbf{r})$ for the hole degrees of freedom. The superconducting order parameter $\Delta(\mathbf{r})e^{i\phi}$ is nonzero only in the superconductor. We will take $\Delta(\mathbf{r}) = \Delta\Theta(z)$, where $\Theta(z) = 1$ if $z > 0$ and 0 otherwise. This step function model is appropriate for tunneling interfaces of s-wave superconductors.[43]

For the single-particle Hamiltonian, we take the simplest model that contains the essential features of the half-metal–superconductor interface,

$$\hat{H} = -\hbar^2\nabla\frac{1}{2m(z)}\nabla - \sum_\sigma \mu_\sigma(z)\hat{P}_\sigma(\mathbf{r}) + \hbar w\delta(z), \tag{11}$$

where

$$m(z) = \begin{cases} m_{\mathrm{H}} & \text{if } z < 0, \\ m_{\mathrm{S}} & \text{if } z > 0, \end{cases} \tag{12}$$

with m_{H} and m_{S} being the effective masses for the half-metal and the superconductor, respectively,

$$\mu_\sigma(z) = \begin{cases} \mu_{\mathrm{H}\sigma} & \text{if } z < 0, \\ \mu_{\mathrm{S}} & \text{if } z > 0, \end{cases} \tag{13}$$

with $\sigma = \uparrow, \downarrow$ and the potentials $\mu_{\mathrm{H}\uparrow}$, $\mu_{\mathrm{H}\downarrow}$, and μ_{S} representing the combined effect of the chemical potential and band offsets for the majority and minority electrons in the half-metal and for the superconductor, respectively, and where w sets the strength of a δ-function potential barrier at the interface. The operators

$$\hat{P}_\uparrow = \tfrac{1}{2} + \tfrac{1}{2}\mathbf{m}(\mathbf{r})\cdot\hat{\boldsymbol{\sigma}}, \quad \hat{P}_\downarrow = \tfrac{1}{2} - \tfrac{1}{2}\mathbf{m}(\mathbf{r})\cdot\hat{\boldsymbol{\sigma}} \tag{14}$$

project onto the majority and minority components, respectively, where $\mathbf{m}(\mathbf{r})$ is a unit vector pointing along the magnetization direction in the half-metal.

The potentials $\mu_{\mathrm{H}\uparrow}$, $\mu_{\mathrm{H}\downarrow}$, and μ_{S} are chosen such that $\mu_{\mathrm{H}\uparrow}$, $\mu_{\mathrm{S}} > 0$, and $\mu_{\mathrm{H}\downarrow} < 0$. As a result, majority states in the half-metal and in the normal state of the superconductor are propagating states, with Fermi wave numbers

$$k_\uparrow = \frac{1}{\hbar}\sqrt{2m_{\mathrm{H}}\mu_{\mathrm{H}\uparrow}}, \quad k_{\mathrm{S}} = \frac{1}{\hbar}\sqrt{2m_{\mathrm{S}}\mu_{\mathrm{S}}}, \tag{15}$$

respectively. The corresponding Fermi velocities are $v_\uparrow = \hbar k_\uparrow/m_{\mathrm{H}}$ and $v_{\mathrm{S}} = \hbar k_{\mathrm{S}}/m_{\mathrm{S}}$, respectively. Minority states in the half-metal are evanescent with wave-function decay rate

$$\kappa_\downarrow = \frac{1}{\hbar}\sqrt{2m_{\mathrm{H}}|\mu_{\mathrm{H}\downarrow}|}. \tag{16}$$

(The wave-function decay rate $\kappa_\downarrow$ is the inverse of the wave-function decay length ξ used in the previous section.) The strength w of the δ-function potential is chosen such that the transmission probability of the interface is much smaller than unity. It is in this limit only, that the step-function model for the superconducting order parameter Δ used in Eq. (9) is valid.[43] We use the Andreev approximation $\Delta \ll \mu_{\mathrm{S}}$ throughout our calculation.

B. Scattering states for $\Delta = 0$

In order to introduce the relevant notation, we first consider solutions of the Bogoliubov–de Gennes equation (9) in the normal state (i.e., with $\Delta = 0$), for a spatially uniform magnetization direction $\mathbf{m} = \mathbf{e}_3$, and at $\varepsilon = 0$. In this case, solutions of the Bogoliubov–de Gennes equation (9) can be written as a product

$$\Psi(\mathbf{r}) = e^{i\mathbf{k}_\parallel\cdot\mathbf{r}}\Psi_{\mathbf{k}_\parallel}(z), \tag{17}$$

where $\mathbf{k}_\parallel = k_x\mathbf{e}_x + k_y\mathbf{e}_y$. For $z < 0$, the spinor wave function $\Psi_{\mathbf{k}_\parallel}$ has the general form

$$\Psi_{\mathbf{k}_\parallel}(z) = \frac{1}{\sqrt{v_{\uparrow z}}}\begin{pmatrix} c_{\mathrm{e}\uparrow}e^{ik_{\uparrow z}z} + c'_{\mathrm{e}\uparrow}e^{-ik_{\uparrow z}z} \\ 0 \\ c_{\mathrm{h}\uparrow}e^{-ik_{\uparrow z}z} + c'_{\mathrm{h}\uparrow}e^{ik_{\uparrow z}z} \\ 0 \end{pmatrix} + \frac{1}{\sqrt{v_{\downarrow z}}}\begin{pmatrix} 0 \\ c_{\mathrm{e}\downarrow}e^{\kappa_{\downarrow z}z} \\ 0 \\ c_{\mathrm{h}\downarrow}e^{\kappa_{\downarrow z}z} \end{pmatrix}, \tag{18}$$

where

$$k_{\uparrow z} = \sqrt{k_\uparrow^2 - |\mathbf{k}_\parallel|^2}, \quad \kappa_{\downarrow z} = \sqrt{\kappa_\downarrow^2 + |\mathbf{k}_\parallel|^2}, \tag{19}$$

and

$$v_{\uparrow z} = \hbar k_{\uparrow z}/m_{\mathrm{H}}, \quad v_{\downarrow z} = \hbar\kappa_{\downarrow z}/m_{\mathrm{H}}. \tag{20}$$

In the superconductor, for $z > 0$, the general form of the spinor wave function is

$$\Psi_{\mathbf{k}_\parallel}(z) = \frac{1}{\sqrt{v_{\mathrm{S}z}}}\begin{pmatrix} d_{\mathrm{e}\uparrow}e^{-ik_{\mathrm{S}z}z} + d'_{\mathrm{e}\uparrow}e^{ik_{\mathrm{S}z}z} \\ d_{\mathrm{e}\downarrow}e^{-ik_{\mathrm{S}z}z} + d'_{\mathrm{e}\downarrow}e^{ik_{\mathrm{S}z}z} \\ d_{\mathrm{h}\uparrow}e^{ik_{\mathrm{S}z}z} + d'_{\mathrm{h}\uparrow}e^{-ik_{\mathrm{S}z}z} \\ d_{\mathrm{h}\downarrow}e^{ik_{\mathrm{S}z}z} + d'_{\mathrm{h}\downarrow}e^{-ik_{\mathrm{S}z}z} \end{pmatrix}, \tag{21}$$

where

$$k_{\mathrm{S}z} = \sqrt{k_{\mathrm{S}}^2 - |\mathbf{k}_\parallel|^2}, \quad v_{\mathrm{S}z} = \hbar k_{\mathrm{S}z}/m_{\mathrm{S}}. \tag{22}$$

The amplitudes appearing in the above equations are related as

$$\begin{pmatrix} c'_{\mathrm{e}\uparrow} \\ d'_{\mathrm{e}\uparrow} \\ c'_{\mathrm{h}\uparrow} \\ d'_{\mathrm{h}\uparrow} \end{pmatrix} = \begin{pmatrix} r & t & 0 & 0 \\ t & r' & 0 & 0 \\ 0 & 0 & r^* & t^* \\ 0 & 0 & t^* & r'^* \end{pmatrix} \begin{pmatrix} c_{\mathrm{e}\uparrow} \\ d_{\mathrm{e}\uparrow} \\ c_{\mathrm{h}\uparrow} \\ d_{\mathrm{h}\uparrow} \end{pmatrix},$$
$$\begin{pmatrix} c_{\mathrm{e}\downarrow} \\ d'_{\mathrm{e}\downarrow} \\ c_{\mathrm{h}\downarrow} \\ d'_{\mathrm{h}\downarrow} \end{pmatrix} = \begin{pmatrix} t_\downarrow & 0 \\ r'_\downarrow & 0 \\ 0 & t^*_\downarrow \\ 0 & r'^*_\downarrow \end{pmatrix} \begin{pmatrix} d_{\mathrm{e}\downarrow} \\ d_{\mathrm{h}\downarrow} \end{pmatrix}, \tag{23}$$

with

$$\begin{aligned} t &= \frac{2\sqrt{v_{\uparrow z} v_{\mathrm{S}z}}}{2iw + v_{\uparrow z} + v_{\mathrm{S}z}}, \\ r &= -1 + t\sqrt{v_{\uparrow z}/v_{\mathrm{S}z}}, \\ r' &= -1 + t\sqrt{v_{\mathrm{S}z}/v_{\uparrow z}}, \\ r'_\downarrow &= -1 + t_\downarrow\sqrt{v_{\mathrm{S}z}/v_{\downarrow z}}, \\ t_\downarrow &= \frac{2\sqrt{v_{\downarrow z} v_{\mathrm{S}z}}}{2iw + iv_{\downarrow z} + v_{\mathrm{S}z}}. \end{aligned} \tag{24}$$

The amplitudes r, r', and t are majority electron reflection and transmission amplitudes of the half-metal–superconductor interface (with the superconductor in the normal state); the amplitude $r'_\downarrow$ is the minority electron reflection amplitude. The coefficient $t_\downarrow$ parametrizes the evanescent wave amplitude for minority electrons in the half-metal. (There is no transmission amplitude for minority electrons.) In terms of these amplitudes, the assumption of a tunneling interface translates to $|t|, |t_\downarrow| \ll 1$.

C. Scattering states for uniform magnetization

We now use the notation established in the previous subsection to construct retarded and advanced scattering states for the half-metal–superconductor interface at finite excitation energy ε. The scattering states will be used for the perturbation-theory calculation of the Andreev reflection amplitudes for a nonuniform magnetization in the next section.

As before, we consider a spatially uniform magnetization direction $\mathbf{m} = \mathbf{e}_3$. For each wave vector $\mathbf{k}_\parallel$, there is an electron-like and a hole-like scattering state, which we label $|\mathbf{k}_\parallel, \mathrm{e}\rangle^{\mathrm{R}}$ and $|\mathbf{k}_\parallel, \mathrm{h}\rangle^{\mathrm{R}}$ for the retarded states and $|\mathbf{k}_\parallel, \mathrm{e}\rangle^{\mathrm{A}}$ and $|\mathbf{k}_\parallel, \mathrm{h}\rangle^{\mathrm{A}}$ for the advanced states. A retarded scattering state is called "electron-like" or "hole-like" if the incoming part is electron-like or hole-like, respectively, whereas one considers the outgoing part of the wave function for an advanced scattering state. In general, the outgoing part of a retarded scattering state will be of mixed electron/hole type, as well as the incoming part of an advanced scattering state. For the states constructed below, however, there is no mixing between electron-like and hole-like parts in the propagating components, since there is no Andreev reflection at an HS interface if the magnetization is uniform. Only the evanescent parts of the scattering states will be of mixed electron/hole type.

The scattering states are constructed from the general form of the spinor wave function $\Psi_{\mathbf{k}_\parallel}(z)$ at finite excitation energy ε and with nonzero superconducting order parameter Δ, which reads

$$\Psi_{\mathbf{k}_\parallel}(z) = \frac{1}{\sqrt{v_{\uparrow z}}} \begin{pmatrix} c_{\mathrm{e}\uparrow} e^{ik_{\uparrow z}(\varepsilon)z} + c'_{\mathrm{e}\uparrow} e^{-ik_{\uparrow z}(\varepsilon)z} \\ 0 \\ c_{\mathrm{h}\uparrow} e^{-ik_{\uparrow z}(-\varepsilon)z} + c'_{\mathrm{h}\uparrow} e^{ik_{\uparrow z}(-\varepsilon)z} \\ 0 \end{pmatrix} + \frac{1}{\sqrt{v_{\downarrow z}}} \begin{pmatrix} 0 \\ c_{\mathrm{e}\downarrow} e^{\kappa_{\downarrow z}(\varepsilon)z} \\ 0 \\ c_{\mathrm{h}\downarrow} e^{\kappa_{\downarrow z}(-\varepsilon)z} \end{pmatrix} \tag{25}$$

for $z < 0$, and

$$\Psi_{\mathbf{k}_\parallel}(z) = \frac{e^{ik_{\mathrm{S}z}z - \kappa_{\mathrm{S}z}(\varepsilon)z}}{\sqrt{v_{\mathrm{S}z}}} \begin{pmatrix} d'_\uparrow \\ d'_\downarrow \\ -d'_\downarrow e^{-i\eta(\varepsilon)-i\phi} \\ d'_\uparrow e^{-i\eta(\varepsilon)-i\phi} \end{pmatrix} + \frac{e^{-ik_{\mathrm{S}z}z - \kappa_{\mathrm{S}z}(\varepsilon)z}}{\sqrt{v_{\mathrm{S}z}}} \begin{pmatrix} d_\uparrow \\ d_\downarrow \\ -d_\downarrow e^{+i\eta(\varepsilon)-i\phi} \\ d_\uparrow e^{+i\eta(\varepsilon)-i\phi} \end{pmatrix} \tag{26}$$

for $z > 0$. Here we defined

$$k_{\uparrow z}(\varepsilon) = k_{\uparrow z} + \varepsilon/\hbar v_{\uparrow z}, \tag{27}$$

$$\kappa_{\downarrow z}(\varepsilon) = \kappa_{\downarrow z} - \varepsilon/\hbar v_{\downarrow z}, \tag{28}$$

$$\eta(\varepsilon) = \arccos(\varepsilon/\Delta), \tag{29}$$

$$\kappa_{\mathrm{S}z}(\varepsilon) = (\sqrt{\Delta^2 - \varepsilon^2})/\hbar v_{\mathrm{S}z}. \tag{30}$$

[In Eqs. (27), (28), and (30) we kept the leading terms in a small-ε expansion only.] Solution of the Bogoliubov–de Gennes equation (9) in the Andreev approximation then gives the following relations between the coefficients:

$$\begin{aligned} c'_{\mathrm{e}\uparrow} &= \left(r + \frac{t^2}{e^{2i\eta(\varepsilon)}r'_\downarrow - r'}\right) c_{\mathrm{e}\uparrow}, \quad c_{\mathrm{h}\downarrow} = \frac{tt_\downarrow e^{i\eta(\varepsilon)-i\phi}}{e^{2i\eta(\varepsilon)}r'_\downarrow - r'} c_{\mathrm{e}\uparrow}, \\ d_\uparrow &= \frac{t}{e^{2i\eta(\varepsilon)}r'_\downarrow - r'} c_{\mathrm{e}\uparrow}, \quad d'_\uparrow = \frac{tr'_\downarrow e^{2i\eta(\varepsilon)}}{e^{2i\eta(\varepsilon)}r'_\downarrow - r'} c_{\mathrm{e}\uparrow}, \\ c'_{\mathrm{h}\uparrow} &= \left(r^* + \frac{t^{*2}}{e^{2i\eta(\varepsilon)}r'^*_\downarrow - r'^*}\right) c_{\mathrm{h}\uparrow}, \quad c_{\mathrm{e}\downarrow} = -\frac{t^*t^*_\downarrow e^{i\eta(\varepsilon)+i\phi}}{e^{2i\eta(\varepsilon)}r'^*_\downarrow - r'^*} c_{\mathrm{h}\uparrow}, \\ d_\downarrow &= -\frac{t^*r'^*_\downarrow e^{i\eta(\varepsilon)+i\phi}}{e^{2i\eta(\varepsilon)}r'^*_\downarrow - r'^*} c_{\mathrm{h}\uparrow}, \quad d'_\downarrow = -\frac{t^* e^{i\eta(\varepsilon)+i\phi}}{e^{2i\eta(\varepsilon)}r'^*_\downarrow - r'^*} c_{\mathrm{h}\uparrow}. \end{aligned} \tag{31}$$

With the help of the above wave functions, we construct the retarded scattering states $|\mathbf{k}_\parallel,\mathrm{e}\rangle^\mathrm{R}$ and $|\mathbf{k}_\parallel,\mathrm{h}\rangle^\mathrm{R}$ as the state with wave function

$$\begin{aligned}\langle\mathbf{r}|\mathbf{k}_\parallel,\mathrm{e}\rangle^\mathrm{R} &= \frac{1}{\sqrt{W_x W_y}}\Psi_{\mathbf{k}_\parallel,\mathrm{e}}(z)e^{i\mathbf{k}_\parallel\cdot\mathbf{r}},\\ \langle\mathbf{r}|\mathbf{k}_\parallel,\mathrm{h}\rangle^\mathrm{R} &= \frac{1}{\sqrt{W_x W_y}}\Psi_{\mathbf{k}_\parallel,\mathrm{h}}(z)e^{i\mathbf{k}_\parallel\cdot\mathbf{r}},\end{aligned} \tag{32}$$

where W_x and W_y are the dimensions of the HS interface in the x and y directions, the spinor wave function $\Psi_{\mathbf{k}_\parallel,\mathrm{e}}(z)$ is given by Eqs. (25) and (26) with $c_{\mathrm{e}\uparrow}=1$, $c_{\mathrm{h}\downarrow}=0$, all other coefficients being determined by Eqs. (31), and the spinor wave function $\Psi_{\mathbf{k}_\parallel,\mathrm{h}}(z)$ is given by Eqs. (25) and (26) with $c_{\mathrm{e}\uparrow}=0$, $c_{\mathrm{h}\downarrow}=1$. Similarly, the advanced scattering states $|\mathbf{k}_\parallel,\mathrm{e}\rangle^\mathrm{A}$ and $|\mathbf{k}_\parallel,\mathrm{h}\rangle^\mathrm{A}$ are then defined as the states for which $c'_{\mathrm{e}\uparrow}=1$, $c'_{\mathrm{h}\downarrow}=0$ and $c'_{\mathrm{e}\uparrow}=0$, $c'_{\mathrm{h}\downarrow}=1$, respectively, again with all other coefficients determined by Eqs. (31). The factors $1/\sqrt{W_x W_y}$ in Eqs. (32) ensure that retarded and advanced scattering states are normalized to unit incoming or outgoing flux in the z direction, respectively. The lengths W_x and W_y do not appear in the final expressions for the Andreev reflection amplitudes. These scattering states are at the basis of the calculation of the Andreev reflection amplitudes in the presence of a nonuniform magnetization, which is described in the next section.

IV. ANDREEV REFLECTION IN THE PRESENCE OF A NONUNIFORM MAGNETIZATION DIRECTION

A. Slow variations of the magnetization direction

A spatial variation of the magnetization direction in the half-metal breaks the remaining symmetries in spin space and allows for Andreev reflection at the half-metal–superconductor interface. Here we consider a continuous and slow variation of the the magnetization direction $\mathbf{m}(\mathbf{r})$. An example of such a continuous change is a domain wall, for which the net change of the magnetization angle is π, smeared out over a length l_d much larger than the microscopic lengths k_S^{-1}, $k_\uparrow^{-1}$, and $\kappa_\downarrow^{-1}$. However, smaller rotation angles are possible, too, e.g., induced by strain at the interface due to lattice mismatches.[44]

To be specific, we choose a right-handed set of unit vectors $\mathbf{e}_1$, $\mathbf{e}_2$, and $\mathbf{e}_3$ in spin space (which need not coincide with the coordinates used for the orbital degrees of freedom) and consider a variation of the magnetization direction $\mathbf{m}$ of the form

$$\mathbf{m}(\mathbf{r}) = (\mathbf{e}_1\cos\phi_\mathrm{m} + \mathbf{e}_2\sin\phi_\mathrm{m})\sin\theta_\mathrm{m}(\mathbf{r}) + \mathbf{e}_3\cos\theta_\mathrm{m}(\mathbf{r}). \tag{33}$$

Such variations of the magnetization direction are sufficient to model domain walls, but they do not allow for certain continuous changes of the magnetization at a fixed polar angle, as it occurs in helical magnets. (The full expressions for arbitrary variations of $\mathbf{m}$ are given in the Appendix.) We then employ a gauge transformation that rotates $\mathbf{m}$ to the $\mathbf{e}_3$ direction,

$$\mathcal{H}\to\mathcal{U}(\mathbf{r})^\dagger\mathcal{H}\mathcal{U}(\mathbf{r}),\quad \mathcal{U}(\mathbf{r}) = \begin{pmatrix} U(\mathbf{r}) & 0\\ 0 & U^*(\mathbf{r})\end{pmatrix}, \tag{34}$$

with

$$U(\mathbf{r}) = e^{i\theta_\mathrm{m}[\mathbf{m}(\mathbf{r})\times\mathbf{e}_3]\cdot\boldsymbol{\sigma}/2\sin\theta_\mathrm{m}}. \tag{35}$$

This gauge transformation adds a spin-dependent gauge potential

$$\mathbf{A}(\mathbf{r}) = i\hbar U^\dagger\nabla U = \frac{\hbar}{2}(\sigma_2\cos\phi_\mathrm{m} - \sigma_1\sin\phi_\mathrm{m})\nabla\theta_\mathrm{m} \tag{36}$$

to the Hamiltonian $\hat{H}$,[45] but it does not affect the singlet superconducting order parameter, since $U^\mathrm{T}i\sigma_2\Delta U = i\sigma_2\Delta$. To lowest order in the rate of change of the angle θ_m we then find that the perturbation $\hat{V}$ to the Hamiltonian $\hat{H}$ reads

$$\hat{V} = i(\sigma_2\cos\phi_\mathrm{m} - \sigma_1\sin\phi_\mathrm{m})\left(\nabla\theta\cdot\frac{\hbar^2}{2m}\nabla + \nabla\frac{\hbar^2}{2m}\cdot\nabla\theta\right). \tag{37}$$

Since we take the length scale l_d for variations of the gradient of the magnetization angle θ_m to be large in comparison to the microscopic length scales $k_\uparrow^{-1}$, k_S^{-1}, and $\kappa_\downarrow^{-1}$, we may neglect spatial variations of the perturbation $\hat{V}$ in the direction parallel to the interface. In this approximation translation symmetry along the interface is preserved (after the gauge transformation) and the scattering matrix $\mathcal{S}(\mathbf{k}'_\parallel,\mathbf{k}_\parallel;\varepsilon)$ is diagonal, see Eq. (3). To lowest order in the rate of change of θ_m, the Andreev reflection amplitudes may then be calculated in perturbation theory. Using the scattering states defined in the previous section, one finds

$$\begin{aligned} r_\mathrm{he}(\mathbf{k}_\parallel,\varepsilon) &= -\frac{i}{\hbar}\,{}^\mathrm{A}\langle\mathbf{k}_\parallel,\mathrm{h},\varepsilon|\mathcal{V}|\mathbf{k}_\parallel,\mathrm{e},\varepsilon\rangle^\mathrm{R},\\ r_\mathrm{eh}(\mathbf{k}_\parallel,\varepsilon) &= -\frac{i}{\hbar}\,{}^\mathrm{A}\langle\mathbf{k}_\parallel,\mathrm{e},\varepsilon|\mathcal{V}|\mathbf{k}_\parallel,\mathrm{h},\varepsilon\rangle^\mathrm{R},\end{aligned} \tag{38}$$

where

$$\mathcal{V} = \begin{pmatrix}\hat{V} & 0\\ 0 & -\hat{V}^*\end{pmatrix}. \tag{39}$$

We now present calculations of the Andreev reflection amplitudes for two special cases: Variation of the angle θ_m in a direction perpendicular to the superconductor interface, as illustrated in Fig. 3(a), and variation of θ_m in a direction parallel to the superconductor interface, which is illustrated in Fig. 3(b). These two cases differ with respect to the symmetries discussed in Sec. II: The rotation symmetry around an axis normal to the interface is preserved in the former case, whereas it is broken in the latter case. We will see that this difference has profound consequences for the Andreev reflection amplitude.

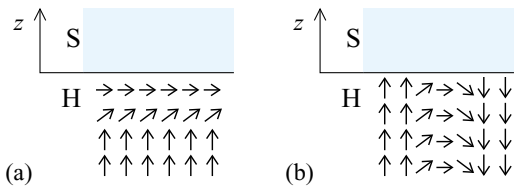

FIG. 3. (Color online) Illustration of a magnetization gradient perpendicular to the HS interface (a) and parallel to the HS interface (b).

A variation perpendicular to the interface is relevant, e.g., if the interface anisotropy at the half-metal–superconductor interface differs from the anisotropy in the bulk of the half-metal. Calculating the Andreev reflection amplitude, we find, to leading orders in $|t|$ and $|t_\downarrow|$,

$$r_{\rm he}(\mathbf{k}_\parallel;\varepsilon) = -\frac{i\varepsilon e^{-i(\phi-\phi_{\rm m})}\Delta}{\kappa_{\downarrow z}\sqrt{\Delta^2-\varepsilon^2}}(\nabla\theta_{\rm m}\cdot\mathbf{e}_z) \times\left[\frac{|tt_\downarrow|^2}{8\sqrt{\Delta^2-\varepsilon^2}} + \frac{\left(v_{\downarrow z}^2-v_{\uparrow z}^2\right){\rm Re}\, tt_\downarrow}{\hbar k_{\uparrow z}\left(v_{\downarrow z}^2+v_{\uparrow z}^2\right)\sqrt{v_{\uparrow z}v_{\downarrow z}}}\right]. \tag{40}$$

The dependence of this result on the interface parameters agrees with what was derived in Sec. II using general considerations. Note that in the limit $\kappa_\downarrow\to\infty$, in which the minority carriers are completely expelled from the half-metal, the Andreev reflection amplitude $r_{\rm he}$ vanishes. The appearance of the azimuthal magnetization angle $\phi_{\rm m}$ as a shift of the superconducting phase ϕ was found previously in Refs. 20,29 for the interface between a magnetic multilayer and a superconductor.

The divergence for $\varepsilon\to\pm\Delta$ in Eq. (40) is an artifact of the expansion in the transmission amplitudes t and $t_\downarrow$ and has to be cut off for $1-(\varepsilon/\Delta)^2\lesssim\max(|t|^4,|tt_\downarrow|^2)$. This means that the immediate vicinity of $\pm\Delta$ has to be excluded from the region of validity of Eq. (40), so that Eq. (40) is valid for $1-(\varepsilon/\Delta)^2\gg\max(|t|^4,|tt_\downarrow|^2)$ only. The same condition will be required for the validity of Eqs. (41) and (44) below, as well as the expressions derived from them. (We note that similar restrictions also apply to an expansion in the transmission coefficient for a normal-metal–superconductor interface, see, e.g., Ref. 39.)

A variation of the magnetization direction in which $\nabla\theta_{\rm m}$ is parallel to the superconductor interface breaks the rotation symmetry around an axis normal to the interface, thus allowing, in principle, for a nonzero Andreev reflection amplitude at the Fermi level $\varepsilon=0$.[32] Here we elaborate on our previous calculation of this effect and generalize the results of Ref. 32 to the case of a finite minority wave function decay rate $\kappa_\downarrow$ in the half-metal. Calculating the Andreev reflection amplitude according to Eq. (38), we then find, again to leading orders in $|t|$ and $|t_\downarrow|$,

$$r_{\rm he}(\mathbf{k}_\parallel;\varepsilon) = -\frac{e^{-i(\phi-\phi_{\rm m})}\Delta}{\sqrt{\Delta^2-\varepsilon^2}}(\nabla\theta_{\rm m}\cdot\mathbf{k}_\parallel) \times\left[\frac{|t|^2}{4k_{{\rm S}z}^2} + \frac{v_{\uparrow z}{\rm Re}\, tt_\downarrow}{\left(k_{\uparrow z}^2+\kappa_{\downarrow z}^2\right)\sqrt{v_{\uparrow z}v_{\downarrow z}}}\right]. \tag{41}$$

The first term in Eq. (41) comes from the overlap integral in Eq. (38) inside the superconductor, whereas the second term comes from the overlap integral in the half-metal. The existence of a finite contribution to $r_{\rm he}$ from inside the superconductor is responsible for the fact that $r_{\rm he}$ remains nonzero in the limit $\kappa_\downarrow\to\infty$ if $\theta_{\rm m}$ varies parallel to the interface. In both cases, the amplitude for the conversion of holes into electrons is given by

$$r_{\rm eh}(\mathbf{k}_\parallel;\varepsilon) = r_{\rm he}(-\mathbf{k}_\parallel;-\varepsilon)^*,$$

as discussed in Sec. II. For a general direction of $\nabla\theta_{\rm m}$, the Andreev reflection amplitudes are the sums of the contributions of Eqs. (40) and (41) above.

We note that the presence of Andreev reflection at the Fermi energy for a domain wall with $\nabla\theta_{\rm m}$ parallel to the interface is accompanied by a nontrivial angle dependence of the Andreev reflection amplitudes $r_{\rm eh}$ and $r_{\rm he}$: If $\nabla\theta_{\rm m}$ is parallel to the interface, $r_{\rm he}$ and $r_{\rm eh}$ are even functions of ε, but odd functions of $\mathbf{k}_\parallel$. On the other hand, if $\nabla\theta_{\rm m}$ is normal to the interface, $r_{\rm he}$ and $r_{\rm eh}$ are odd functions of ε, but even functions of $\mathbf{k}_\parallel$. Similar behavior has been noticed previously for the anomalous Green functions.[27,46]

B. Spin-active interfaces

As a second example of a spatially varying magnetization direction, we now investigate a simplified model of a thin ferromagnetic or half-metallic layer located at the interface, the magnetization of which is misaligned with respect to the bulk of the half-metal. In this model of what is more generally referred to as a "spin-active interface,"[24–27,38] we take the magnetization direction to be the unit vector $\mathbf{e}_3$ in the entire half-metal and consider a perturbation to the Hamiltonian $\hat{H}$ of the form

$$\hat{V} = \tilde{h}\tilde{\mathbf{m}}\cdot\hat{\boldsymbol{\sigma}}\,\delta(z), \tag{42}$$

where

$$\tilde{\mathbf{m}} = (\mathbf{e}_1\cos\phi_{\rm m}+\mathbf{e}_2\sin\phi_{\rm m})\sin\theta_{\rm m}+\mathbf{e}_3\cos\theta_{\rm m}. \tag{43}$$

Spin-flip Andreev reflection at such "spin-active" HS interfaces has been considered previously in Refs. 27–29. Using Eq. (38) to calculate the Andreev reflection amplitude to first order in $\tilde{h}$ and taking the limit of a tunneling interface, $|tt_\downarrow|^2\ll 1$, we then find

$$r_{\rm he}(\mathbf{k}_\parallel;\varepsilon) = -\frac{i\varepsilon\Delta\tilde{h}|tt_\downarrow|^2e^{-i(\phi-\phi_{\rm m})}\sin\theta_{\rm m}}{2\hbar v_{\downarrow z}(\Delta^2-\varepsilon^2)}. \tag{44}$$

The proportionality to the square of the tunneling probability is in agreement with the general considerations of Sec. II. The opposite limit of an ideal interface ($|t|=|t_\downarrow|=1$) was considered in Ref. 29.

C. Applications: Conductance and Josephson current

The Andreev reflection amplitudes $r_{\rm he}$ and $r_{\rm eh}$ enter directly into the calculation of the subgap conductance G of an HS junction and the Josephson current I of an SHS junction. Below, we calculate G and I for the two special cases of a magnetization gradient $\nabla\theta_{\rm m}$ that is perpendicular and parallel to the interface considered above. To be precise, in the first case we take $\theta_{\rm m}$ to be a function of the coordinate z only, with a finite derivative $d\theta_{\rm m}/dz=l_{\rm d}^{-1}$ at the interface, whereas in the second case we take $\theta_{\rm m}$ to be a function of the coordinate x only, with the x dependence given by the common domain wall profile[47]

$$\theta_{\rm m}(x) = \arctan[\sinh(\pi x/l_{\rm d})]. \tag{45}$$

Thus, in both cases $l_{\rm d}$ is the length scale related to the rate of change of the magnetization angle $\theta_{\rm m}$.

Even for our simplified model Hamiltonian, the number of parameters in the expressions for the Andreev reflection amplitudes is so large, that no compact expressions for the conductance can be obtained. We therefore make the simplifying assumptions that $m_{\rm H} = m_{\rm S} = m$ and that $w, \Delta/\hbar k_\uparrow \ll v_\uparrow \ll v_\downarrow, v_{\rm S}$. In this limit, one has $t \approx 2\sqrt{v_{\uparrow z}/v_{\rm S}}$ and $t_\downarrow \approx 2\sqrt{v_\downarrow v_{\rm S}}/(iv_\downarrow + v_{\rm S})$, so that the interface transmission coefficients are much smaller than unity even in the absence of the δ-function potential barrier.

The subgap conductance $G(V)$ is given by the expression[42]

$$G(V) = \frac{2e^2}{h}\frac{1}{4\pi^2}\int dxdy \int_{k_\parallel<k_\uparrow} d\mathbf{k}_\parallel |r_{\rm he}(\mathbf{k}_\parallel, eV)|^2, \quad (46)$$

where the integration over the coordinates x and y extends along the HS interface. (The appearance of a reflection amplitude $r_{\rm he}$ that simultaneously depends on the momentum $\mathbf{k}_\parallel$ and position at the interface is justified by the slow variation of the magnetization direction with position—see the discussion in Sec. IV A.) In the limit described in the paragraph following Eq. (45), one then finds the subgap conductance

$$G(V) = g_1 W_x W_y \left(\frac{eV\Delta}{\Delta^2 - (eV)^2}\right)^2 \quad (47)$$

for the first case of $\nabla\theta_{\rm m}$ perpendicular to the HS interface, where

$$g_1 = \frac{2e^2}{h}\frac{1}{l_{\rm d}^2}\frac{v_\uparrow^4}{2\pi\left(v_\downarrow^2 + v_{\rm S}^2\right)^2} \quad (48)$$

has the dimensions of conductance per area. For the second special case of $\nabla\theta_{\rm m}$ parallel to the HS interface one finds

$$G(V) = g_2 W_y l_{\rm d}\pi \frac{\Delta^2}{\Delta^2 - (eV)^2} \quad (49)$$

with

$$g_2 = \frac{2e^2}{h}\frac{1}{l_{\rm d}^2}\frac{v_\uparrow^6}{24\pi v_\downarrow^4 v_{\rm S}^2}\left(\frac{v_\downarrow^2}{v_{\rm S}^2} + \frac{4v_{\rm S}^2}{v_\downarrow^2 + v_{\rm S}^2}\right)^2. \quad (50)$$

The main difference between the two cases is that $G(V)$ is proportional to V^2 and to $W_x W_y/l_{\rm d}^2$ in the former scenario,[29,36] whereas in the second scenario $G(V)$ approaches a constant in the limit $V \to 0$, which is proportional to $W_y/l_{\rm d}$.[32]

For the first case of $\nabla\theta_{\rm m}$ perpendicular to the interface, a deviation from this asymptotic voltage dependence occurs in the limit of extremely low voltages or, alternatively, in the limit of a strong tunnel barrier at the HS interface. In that case, the Andreev reflection amplitude $r_{\rm he}$ is dominated by the second term in Eq. (40), which diverges for angles of incidence close to $\pi/2$. This divergence is an artifact of the Andreev approximation, and the validity of Eq. (40) is restricted to those angles of incidence for which $\varepsilon \ll \hbar^2 k_{\uparrow z}^2/2m$. Cutting off the resulting logarithmic divergence of the conductance divergence, while otherwise employing the same approximations as before, gives

$$G \sim 2g_1 W_x W_y \frac{(eV\Delta)^2 v_{\rm S}^2}{\mu_\uparrow^2(\Delta^2 - (eV)^2)v_\downarrow^2}\ln\frac{\mu_\uparrow}{|eV|}. \quad (51)$$

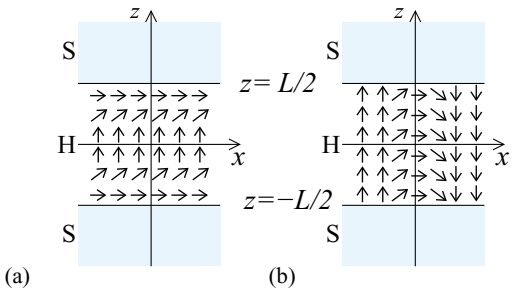

FIG. 4. (Color online) Schematic of an SHS junction with a magnetization gradient perpendicular to the HS interfaces (a) or parallel to the HS interface (b). The magnetization angle $\theta_{\rm m}$ is chosen to be a symmetric function of z.

Equation (51) replaces Eq. (47) for voltages that are low enough that the conductance of Eq. (51) exceeds that of Eq. (47). However, it should be noted that effects not taken into account here, such as scattering off impurities near the HS interface, are expected to give rise to a finite value of G in the limit $V \to 0$, which will in all practical cases mask the asymptotic logarithmic voltage dependence of Eq. (51).

The second application we consider is the Josephson current in an SHS junction. We consider the geometry shown in Fig. 4. The superconductors occupy the space $z > L/2$ and $z < -L/2$, and the phases of the order parameters of the two superconductors are $\phi/2$ and $-\phi/2$, respectively. We consider the so-called "long-junction limit" of junction length $L \gg \hbar v_\uparrow/\Delta$ and restrict our discussion to the temperature range $\hbar v_\uparrow/L \ll k_{\rm B}T \ll \Delta$. In this case, the Josephson current in an SHS junction without impurity scattering is given by the expression[40,41]

$$I = -\frac{4ek_{\rm B}T}{\hbar}\frac{1}{4\pi^2}\int dxdy\frac{d}{d\phi}\int_{k_\parallel<k_\uparrow} d\mathbf{k}_\parallel e^{-2\pi k_{\rm B}TL/\hbar v_{\uparrow z}} \times {\rm Re}\, r_{\rm eh}(\mathbf{k}_\parallel, i\pi k_{\rm B}T) r'_{\rm he}(\mathbf{k}_\parallel, i\pi k_{\rm B}T), \quad (52)$$

where $r_{\rm eh}$ is the Andreev reflection amplitude for the upper HS interface and $r'_{\rm he}$ is the Andreev reflection amplitude for the lower HS interface. In Eq. (52), the Andreev reflection amplitudes are taken at the interface positions $(x \pm Lk_x/2k_{\uparrow z}, y \pm Lk_y/2k_{\uparrow z}, \pm L/2)^{\rm T}$. We take periodic boundary conditions in the x and y directions, which is a good approximation if the junction length $L \ll W_x, W_y$. We further assume that the magnetization profile is symmetric with respect to a reflection in the plane $z = 0$, $\theta_{\rm m}(z) = \theta_{\rm m}(-z)$. With this assumption, $r'_{\rm he}(\mathbf{k}_\parallel, \varepsilon) = r_{\rm he}(\mathbf{k}_\parallel, \varepsilon)e^{i\phi}$. We then find the Josephson current

$$I = \frac{8(\pi k_{\rm B}T)^2\hbar v_\uparrow g_1 W_x W_y}{e\Delta^2 L^2} e^{-2\pi k_{\rm B}TL/\hbar v_\uparrow}\sin\phi \quad (53)$$

for the first case ($\nabla\theta_{\rm m}$ perpendicular to the interface, as in Fig. 4(a), where we omitted corrections that are small in the limit $k_{\rm B}T \gg \hbar v_\uparrow/L$. For the second case ($\nabla\theta_{\rm m}$ parallel to the interface, as in Fig. 4(b), one finds

$$I = -\frac{24(\hbar v_\uparrow)^2 g_2 W_y l_{\rm d}}{ek_{\rm B}TL^2} e^{-2\pi k_{\rm B}TL/\hbar v_\uparrow} \times F\left(\hbar v_\uparrow \pi L/k_{\rm B}T l_{\rm d}^2\right)\sin\phi, \quad (54)$$

where the function F is defined as

$$F(a) = \frac{2}{\sqrt{\pi a^3}} \int d\zeta \frac{\zeta^3 e^{-\zeta^2/a}}{\sinh \zeta} \tag{55}$$

and has the limits $F(0) = 1$ and $F(a) \sim \pi^{7/2}/2a^{3/2}$ for $a \gg 1$. The qualitatively different temperature and junction length dependences of these expressions clearly distinguish the two different magnetization profiles in the half-metal.

V. THIN FILM GEOMETRY

A. Andreev reflection amplitudes

A modification of the scattering problem arises in a lateral contact geometry as in Fig. 1(a). For this geometry a formulation with scattering states describing quasiparticles moving in the plane of the half-metallic film is more relevant than the formulation of the previous sections in terms of scattering states of quasiparticles incident on the HS interface.

The geometry we consider is shown in detail in Fig. 5. As before, the half-metal–superconductor interface is the plane $z = 0$. The superconductor occupies the half-space $z > 0$, whereas the half-metallic film is in the region $-d < z < 0$. The Hamiltonian is given by Eq. (9), and hard-wall boundary conditions are applied at $z = -d$. We choose our coordinates such, that (locally) the magnetization direction does not depend on the coordinate y, so that the wave-vector component k_y is conserved. As in the previous sections, we consider the limit of a tunneling interface, and present our results to leading order in the transmission probability.

We first construct the scattering states in the presence of a uniform magnetization direction $\mathbf{m} = \mathbf{e}_3$. With the help of periodic boundary conditions in the y direction with period W_y, the scattering states are normalized to unit flux in the x direction. There are electron-like and hole-like scattering states $|\mathbf{k}_\perp s;\mathrm{e}\rangle$ and $|\mathbf{k}_\perp s;\mathrm{h}\rangle$, each labeled by the discrete wave-vector components $\mathbf{k}_\perp = (0,k_y,k_{\uparrow z,\mathrm{e}})^{\mathrm{T}}$ and $\mathbf{k}_\perp = (0,k_y,k_{\uparrow z,\mathrm{h}})^{\mathrm{T}}$ of the majority quasiparticles in H and by the integers $s = \pm 1$ for indicates scattering states propagating in the positive ($s = 1$) and negative ($s = -1$) x direction. Because of the hard-wall boundary conditions at $z = -d$, only $k_{\uparrow z} > 0$ need to be considered. In the limit $\kappa_\downarrow d \gg 1$ the hard-wall boundary conditions at $z = -d$ are inconsequential for the minority carriers, and the corresponding wave functions read

$$\begin{aligned}
\Psi_{\mathbf{k}_\perp s,\mathrm{e}}(\mathbf{r}) &= -i\sqrt{\frac{v_{\uparrow z}}{2v_{\uparrow x}W_y d}}\Psi_{\mathbf{k}_\parallel,\mathrm{e}}(z)\, e^{ik_x(\varepsilon)sx+ik_y y},\\
\Psi_{\mathbf{k}_\perp s,\mathrm{h}}(\mathbf{r}) &= i\sqrt{\frac{v_{\uparrow z}}{2v_{\uparrow x}W_y d}}\Psi_{\mathbf{k}_\parallel,\mathrm{h}}(z)\, e^{-ik_x(-\varepsilon)sx+ik_y y},
\end{aligned} \tag{56}$$

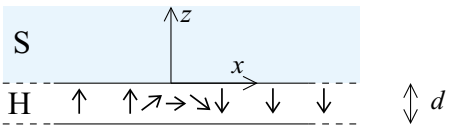

FIG. 5. (Color online) Illustration of the thin-film geometry. The coordinates are chosen such that the magnetization direction does not change in the y direction (perpendicular to the plane of the drawing).

where $\Psi_{\mathbf{k}_\parallel,\mathrm{e}}(z)$ and $\Psi_{\mathbf{k}_\parallel,\mathrm{h}}(z)$ are given in Eq. (32),

$$k_x(\varepsilon) = \sqrt{k_\uparrow^2 - k_{\uparrow z}^2 - k_y^2} + \varepsilon/\hbar v_{\uparrow x}, \tag{57}$$

and the allowed wave numbers $k_{\uparrow z}$ are determined from the condition that the wave functions vanish at $z = -d$, which implies the condition [compare with Eq. (31)]

$$2k_{\uparrow z,\mathrm{e}}d + \pi - \arg\left(r + \frac{t^2}{e^{2i\eta}r'_\downarrow - r'}\right) = 2\pi n_z, \tag{58}$$

for electron-like scattering states, and analogously for hole-like states

$$2k_{\uparrow z,\mathrm{h}}d + \pi - \arg\left(r^* + \frac{t^{*2}}{e^{2i\eta}r'^*_\downarrow - r'^*}\right) = 2\pi n_z, \tag{59}$$

where $n_z = 1,2,\ldots$. In the limit of a tunneling interface, one has $r \to -1$ and $|t| \ll 1$, so that these conditions simplify to

$$k_{\uparrow z} = \frac{\pi n_z}{d} + \mathcal{O}(|t|), \quad n_z = 1,2,\ldots. \tag{60}$$

For the purposes of our calculations, higher-order terms in $|t|$ need to be kept in order to find a finite overlap between the different scattering states, however. The normalization factors in Eq. (56) are valid in the limit of a tunneling interface only.

We now consider the effect of a region in which the magnetization direction is not spatially uniform. In this case, scattering between the electron-like and hole-like quasiparticle states is possible. To lowest order in the rate of change of the magnetization direction, the Andreev reflection amplitudes $r_{\mathrm{he}}^{\mathrm{eff}}$ and $r_{\mathrm{eh}}^{\mathrm{eff}}$ for a quasiparticle incident on a region of nonuniform magnetization can be calculated in perturbation theory as

$$\begin{aligned}
r_{\mathrm{he}}^{\mathrm{eff}}(\mathbf{k}'_\perp s',\mathbf{k}_\perp s;\varepsilon) &= -\frac{i}{\hbar}\langle \mathbf{k}'_\perp s';\mathrm{h}|\mathcal{V}|\mathbf{k}_\perp s;\mathrm{e}\rangle,\\
r_{\mathrm{eh}}^{\mathrm{eff}}(\mathbf{k}'_\perp s',\mathbf{k}_\perp s;\varepsilon) &= -\frac{i}{\hbar}\langle \mathbf{k}'_\perp s';\mathrm{e}|\mathcal{V}|\mathbf{k}_\perp s;\mathrm{h}\rangle,
\end{aligned} \tag{61}$$

where $\mathcal{V}$ is given in Eqs. (37) and (39) above. With these equations, the problem of calculating Andreev reflection coefficients is brought into a form similar to that of the previous section.

In principle, the perturbation $\mathcal{V}$ depends on the coordinate z, even if the magnetization angle θ_{m} does not. [This can be seen from Eq. (37).] Because of this, the scattering matrix need not be diagonal in the transverse wave vector $\mathbf{k}_\perp$. However, if the length scale l_{d} for variations of the gradient $\nabla\theta_{\mathrm{m}}$ in the x direction (i.e., in the plane of the thin film) is large in comparison to the film thickness d, the resulting conservation of the momentum components k_x and k_y up to shifts of order $1/l_{\mathrm{d}} \ll 1/d$, together with energy conservation, constrains the possible values of the transverse momentum $k_{\uparrow z}$. If, in addition, the film thickness d is much smaller than the superconducting coherence length $\xi_{\mathrm{S}} = \hbar v_{\mathrm{S}}/\Delta$, one then finds that the off-diagonal elements of the Andreev reflection amplitude $r_{\mathrm{he}}^{\mathrm{eff}}(\mathbf{k}'_\perp s',\mathbf{k}_\perp,s;\varepsilon)$ are much smaller than the diagonal elements, so that one may set

$$\begin{aligned}
r_{\mathrm{he}}^{\mathrm{eff}}(\mathbf{k}'_\perp s',\mathbf{k}_\perp s;\varepsilon) &= r_{\mathrm{he}}^{\mathrm{eff}}(\mathbf{k}_\perp,s;\varepsilon)\delta_{\mathbf{k}'_\perp,\mathbf{k}_\perp}\delta_{s',-s},\\
r_{\mathrm{eh}}^{\mathrm{eff}}(\mathbf{k}'_\perp s',\mathbf{k}_\perp s;\varepsilon) &= r_{\mathrm{eh}}^{\mathrm{eff}}(\mathbf{k}_\perp,s;\varepsilon)\delta_{\mathbf{k}'_\perp,\mathbf{k}_\perp}\delta_{s',-s}.
\end{aligned} \tag{62}$$

(The Kronecker delta $\delta_{s',-s}$ follows from the conservation of k_x in this limit.) This is the case that we consider in the remainder of this section.

We now give explicit expressions for the case that the magnetization direction $\mathbf{m}$ has the spatial dependence (33) with θ_m a function of x and z only. In that case one finds

$$r_{he}^{\rm eff}(\mathbf{k}_\perp s;\varepsilon) = \frac{v_{\uparrow z}}{2v_{\uparrow x}d}\int dx r_{he}(x;\mathbf{k}_\parallel;\varepsilon)e^{2i\varepsilon s x/\hbar v_{\uparrow x}}, \quad (63)$$

where $r_{he}(x;\mathbf{k}_\parallel;\varepsilon)$ is the Andreev reflection amplitude of Sec. IV, evaluated with the magnetization gradient $\nabla\theta_m$ at position x. The prefactor $v_{\uparrow z}/2v_{\uparrow x}d$ in Eq. (63) expresses the geometric enhancement of the reflection amplitude from the coherent superposition of multiple reflections at the half-metal–superconductor interface.[32] The complex exponential factor accounts for the phase differences acquired by electrons and holes between these reflections. The in-plane wave vector $\mathbf{k}_\parallel = sk_x(0)\mathbf{e}_x + k_y\mathbf{e}_y$; the small difference between the wave number $k_x(\varepsilon)$ of the incoming electron and the wave number $k_x(-\varepsilon)$ of the Andreev reflected hole is inconsequential for the calculation of r_{he} in the Andreev approximation $k_S\xi_S \gg 1$. The corresponding hole-to-electron amplitude r_{eh} is

$$r_{eh}(\mathbf{k}_\perp s;\varepsilon) = r_{he}(\bar{\mathbf{k}}_\perp s;-\varepsilon)^*, \quad (64)$$

where $\bar{\mathbf{k}}_\perp = (0,-k_y,k_z)^{\rm T}$.

We now discuss the cases of a magnetization gradient $\nabla\theta_m$ parallel and perpendicular to the HS interface separately, see Fig. 6 . If $\nabla\theta_m$ is parallel to the HS interface, as is relevant for a domain wall in H, the range of x coordinates for which $\nabla\theta_m$ differs appreciably from zero typically has a finite size $\sim l_d$. In this situation the effective Andreev reflection amplitudes $r_{he}^{\rm eff}$ and $r_{eh}^{\rm eff}$ describe the Andreev reflection of quasiparticles off the region of nonuniform magnetization (i.e., off the domain wall). If l_d is much smaller than the superconducting coherence length ξ_S, the x dependence of the complex exponential $e^{2i\varepsilon x/\hbar v_{\uparrow x}}$ in Eq. (63) can be neglected. Since $r_{he}(x;\mathbf{k}_\parallel;\varepsilon)$ is proportional to $d\theta_m/dx$, the integral over x gives the total change $\delta\theta_m$ of the magnetization angle θ_m, and one finds[32]

$$r_{he}^{\rm eff}(\mathbf{k}_\perp s;\varepsilon) = -\frac{v_{\uparrow z}e^{-i(\phi-\phi_m)}sk_x(0)\Delta}{2v_{\uparrow x}d\sqrt{\Delta^2-\varepsilon^2}}\delta\theta_m \times\left[\frac{|t|^2}{4k_{Sz}^2} + \frac{v_{\uparrow z}\mathrm{Re}\,tt_\downarrow}{(k_{\uparrow z}^2+\kappa_{\downarrow z}^2)\sqrt{v_{\uparrow z}v_{\downarrow z}}}\right]. \quad (65)$$

In this limit, the Andreev reflection amplitude no longer depends on the size l_d of the domain wall, nor on the precise x dependence of the magnetization angle θ_m.[32] In the opposite limit that the domain wall size l_d is large in comparison to the superconducting coherence length, the reflection amplitude at

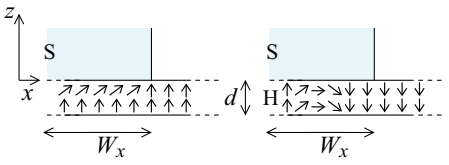

FIG. 6. (Color online) Illustration of a lateral HS contact with a magnetization gradient that is perpendicular to the HS interface (left) or perpendicular to the HS interface (right).

$\varepsilon = 0$ is still given by Eq. (65) above, but Andreev reflection is suppressed for excitation energies ε above the Thouless energy $E_{l_d} = \hbar v_{\uparrow x}/l_d$ of the domain wall. The precise functional form of the suppression depends on the domain wall profile. For the domain wall profile of Eq. (45) the suppression at finite excitation energy ε is by a factor $1/\cosh(\varepsilon l_d/\hbar v_{\uparrow x})$.

If, on the other hand, $\nabla\theta_m$ is perpendicular to the interface, as is the case, e.g., if the interface anisotropy at the HS interface differs from the bulk anisotropy in H, or for a spin-active interface, the region of nonuniform magnetization typically extends along the entire length W_x of the contact. For energies ε below the Thouless energy $\hbar v_\uparrow/W_x$ of the contact one then finds the effective Andreev reflection amplitudes

$$r_{he}^{\rm eff}(\mathbf{k}_\perp s;\varepsilon) = -\frac{i\varepsilon e^{-i(\phi-\phi_m)}v_{\uparrow z}W_x\Delta(\partial\theta_m/\partial z)}{2\kappa_{\downarrow z}v_{\uparrow x}d\sqrt{\Delta^2-\varepsilon^2}} \times\left[\frac{|tt_\downarrow|^2}{8\sqrt{\Delta^2-\varepsilon^2}} + \frac{(v_{\downarrow z}^2-v_{\uparrow z}^2)\mathrm{Re}\,tt_\downarrow}{\hbar k_{\uparrow z}(v_{\downarrow z}^2+v_{\uparrow z}^2)\sqrt{v_{\uparrow z}v_{\downarrow z}}}\right] \quad (66)$$

for the case of interface anisotropy and

$$r_{he}^{\rm eff}(\mathbf{k}_\perp s;\varepsilon) = -\frac{i\varepsilon\tilde{\hbar}v_{\uparrow z}W_x\Delta|tt_\downarrow|^2e^{-i(\phi-\phi_m)}\sin\theta_m}{4\hbar v_{\downarrow z}v_{\uparrow x}d(\Delta^2-\varepsilon^2)} \quad (67)$$

for the case of a spin-active interface. At finite excitation energy ε, the Andreev reflection amplitudes are suppressed by a factor $(\hbar v_{\uparrow x}/\varepsilon W_x)\sin(W_x\varepsilon/\hbar v_{\uparrow x})e^{i\varepsilon W_x/\hbar v_{\uparrow x}}$ with respect to the expressions shown above.

B. Applications: Conductance and Josephson current

As an application, we again consider the conductance of a lateral HS junction and the Josephson current in a lateral SHS junction. We again consider a setup in which that the magnetization angle θ_m depends on the x and z coordinates only, and present results for the cases that the gradient $\nabla\theta_m$ is perpendicular and parallel to the interface, see Fig. 6.

The expressions for conductance and Josephson current are the same as those in Sec. IV C, but with the Andreev reflection amplitudes r_{he} and r_{eh} replaced by $r_{he}^{\rm eff}$ and $r_{eh}^{\rm eff}$, respectively. For the subgap conductance, one thus finds

$$G(V) = \frac{2e^2}{h}\frac{W_y d}{4\pi^2}\int_{k_\perp<k_\uparrow} d\mathbf{k}_\perp\left|r_{he}^{\rm eff}(\mathbf{k}_\perp,eV)\right|^2, \quad (68)$$

where the Andreev reflection amplitude $r_{he}^{\rm eff}(\mathbf{k}_\perp;\varepsilon)$ is for quasiparticles incident from the right, see Fig. 6. Considering the same magnetization profiles and the same limiting case for the parameters appearing in the microscopic expressions for r_{he} as in Sec. IV C, we find that the subgap conductance of a lateral HS junction is

$$G(V) = \frac{g_1 W_y l_d^2}{32d}\left[\frac{\hbar v_\uparrow\Delta}{l_d(\Delta^2-(eV)^2)}\right]^2 \quad (69)$$

with g_1 given by Eq. (48) above, if $\nabla\theta_m$ is perpendicular to the HS interface. Equation (69) is valid for voltages $eV \gg \hbar v_\uparrow/W_x$ that are above the Thouless energy of the contact. We note that in a sufficiently wide lateral contact (such that the condition $eV \gg \hbar v_\uparrow/W_x$ is met for all bias voltages of interest), there is no suppression of the subgap conductance

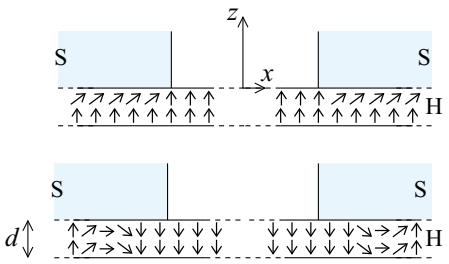

FIG. 7. (Color online) Illustration of a lateral SHS junction with a spatially nonuniform magnetization in the half metal. Two magnetization profiles are considered in the text: the gradient $\nabla\theta_m$ of the magnetization angle perpendicular to the HS interface (top) and parallel to the HS interface (bottom).

at low bias because of the constructive interference of multiple reflections off the HS interface, even if the magnetization gradient is perpendicular to the interface. For the case that $\nabla\theta_m$ is parallel to the interface we find

$$G(V) = \frac{3\pi^2 g_2 W_y l_d^2}{16d} \frac{\Delta^2}{\Delta^2 - (eV)^2} F(eV l_d/\hbar v_\uparrow). \quad (70)$$

Here g_2 is given by Eq. (50) above and the function F is defined as

$$F(a) = 6\int_1^\infty d\zeta \frac{(\zeta^2-1)^2}{\zeta^7 \cosh^2(a\zeta)}, \quad (71)$$

and has the limits $F(0) = 1$ and $F(a) \sim 24e^{-2a}/a^3$ if $a \gg 1$.

For the Josephson current we consider a lateral junction as shown schematically in Fig. 7 . In terms of the effective reflection amplitudes r_{eh}^{eff} and r_{he}^{eff}, the Josephson current at high temperatures $\hbar v_\uparrow/L$, $\hbar v_\uparrow/W_x \ll k_B T \ll \Delta$ is given by the expression

$$I = -\frac{4ek_BT}{\hbar}\frac{W_y d}{4\pi^2}\frac{d}{d\phi}\int_{k_\perp<k_\uparrow} d\mathbf{k}_\perp e^{-2\pi k_B T L/\hbar v_{\uparrow x}} \times \mathrm{Re}\, r_{eh}^{eff}(\mathbf{k}_\perp, i\pi k_B T) r_{he}^{eff}(\mathbf{k}_\perp, i\pi k_B T)', \quad (72)$$

where $r_{he}^{eff}(\mathbf{k}_\perp,\varepsilon)'$ is the Andreev amplitude for the right contact, see Fig. 7. As in Sec. IV C, we consider a symmetric spatial dependence of the magnetization angle, $\theta_m(x) = \theta_m(-x)$, so that the Andreev reflection amplitudes at the right and left contacts are related as $r_{eh}^{eff}(\mathbf{k}_\perp;\varepsilon)' = r_{eh}^{eff}(\mathbf{k}_\perp;\varepsilon)$. If the magnetization gradient is perpendicular to the HS interface, one then finds

$$I = \frac{3W_y g_1 (\hbar v_\uparrow)^5}{8\pi^2 de (k_B T)^2 L^3 \Delta^2} e^{-2\pi k_B T L/\hbar v_\uparrow} \sin\phi, \quad (73)$$

whereas

$$I = \frac{9 g_2 W_y l_d^2 (\hbar v_\uparrow)^3}{2de(k_B T)^2 L^3} e^{-2\pi k_B T L/\hbar v_\uparrow} \sin\phi \quad (74)$$

if the magnetization gradient is parallel to the HS surface, where g_1 and g_2 are given in Eqs. (48) and (50). The length L in Eq. (73) is the distance between the superconducting contacts, while the length L in Eq. (74) is the distance between the domain walls, which may be slightly larger. Equation (74) is derived for the temperature range $\hbar v_\uparrow/L \ll k_B T \ll \hbar v_\uparrow/l_d$. (If $k_B T \gtrsim \hbar v_\uparrow/l_d$, the Josephson current is dominated by the tail of the domain wall at the edge of the lateral contact, and no simple expression can be given.) We thus conclude that in a lateral contact the cases of parallel and perpendicular magnetization gradients results in remarkably similar temperature and length dependences of the Josephson current in the long junction limit.

VI. GREEN FUNCTIONS

Most of the existing theoretical literature on the superconducting proximity effect in ferromagnets and half-metals makes use of the Green function approach, with or without a quasiclassical approximation. In the Green function approach, the induced superconducting correlations in the half-metal are characterized using the "anomalous Green function". The symmetries of this Green function in the spin, orbital, and, in particular, frequency domains are used to classify the various forms of the proximity effect.[3,6,27,46] In this section, we investigate the relation between the scattering approach used here and the Green function approach. (The symmetry in the frequency domain does not play an important role for the scattering approach, because all information is encoded in "retarded" structures in the scattering approach.)

The fundamental equation for the Green function $\mathcal{G}(\mathbf{r},\mathbf{r}';i\Omega)$ is the Gorkov equation

$$(i\Omega - \mathcal{H})\mathcal{G}(\mathbf{r},\mathbf{r}';i\Omega) = \delta(\mathbf{r}-\mathbf{r}'), \quad (75)$$

where $\mathcal{H}$ is the Bogoliubov-de Gennes Hamiltonian of Eq. (9) and Ω the Matsubara frequency. Like the Hamiltonian $\mathcal{H}$, the Green function $\mathcal{G}$ has a 4×4 matrix structure, corresponding to the electron/hole and majority/minority spin degrees of freedom. The anomalous Green function is the electron-hole (eh) block of $\mathcal{G}$. In a half-metal, only the majority component is relevant, so one has

$$F(\mathbf{r},\mathbf{r}';i\Omega) = \mathcal{G}_{e\uparrow,h\uparrow}(\mathbf{r},\mathbf{r}';i\Omega). \quad (76)$$

We first calculate the anomalous Green function $F(\mathbf{r},\mathbf{r}';i\Omega)$ in the vicinity of the interface between a semi-infinite half-metal and a superconductor. This is the geometry considered in Sec. IV. In order to calculate $F(\mathbf{r},\mathbf{r}';i\Omega)$ we Fourier transform the Gorkov equation (75) to the coordinates x and y, and solve the remaining one-dimensional problem using the solutions of the Bogoliubov–de Gennes equation calculated in Sec. IV. For $\Omega > 0$ and coordinates z, $z' < 0$ (i.e., for coordinates inside the half-metal), this procedure expresses the anomalous Green function $F(\mathbf{r},\mathbf{r}';i\Omega)$ in terms of the (outgoing) electron component of the exact hole-like retarded scattering state, and one finds

$$F(\mathbf{r},\mathbf{r}';i\Omega) = \frac{1}{(2\pi)^2}\int dk_x dk_y \times \frac{e^{-ik_z(z-z')+ik_x(x-x')+ik_y(y-y')-|\Omega|(|z|+|z'|)}}{i\hbar v_{\uparrow z}} \times r_{eh}(\mathbf{k};i\Omega), \quad \Omega>0, \quad (77)$$

where

$$k_z = \sqrt{k_\uparrow^2 - k_x^2 - k_y^2}. \quad (78)$$

Similarly, for $\Omega < 0$, the anomalous Green function $F(\mathbf{r},\mathbf{r}';i\Omega)$ is found to be proportional to the (incoming)

electron component of the exact hole-like advanced scattering state,

$$F(\mathbf{r},\mathbf{r}';i\Omega) = -\frac{1}{(2\pi)^2\hbar}\int dk_x dk_y \times \frac{e^{ik_z(z-z')+ik_x(x-x')+ik_y(y-y')-|\Omega|(|z|+|z'|)}}{i\hbar v_{\uparrow z}} \times r_{\rm he}(\mathbf{k}_\parallel;i|\Omega|)^*, \quad \Omega<0. \tag{79}$$

These expressions can be cast in the form

$$F(\mathbf{r},\mathbf{r}';i\Omega)=\frac{1}{2(2\pi)^2 i}\int d\mathbf{k} e^{i\mathbf{k}\cdot(\mathbf{r}-\mathbf{r}')} f(\mathbf{k},\mathbf{R};i\Omega)\delta(\varepsilon_k-\mu_{\rm H\uparrow}), \tag{80}$$

where $\mathbf{R}=\frac{1}{2}(\mathbf{r}+\mathbf{r}')$, $\varepsilon_k=\hbar^2k^2/2m_{\rm H}$, and

$$f(\mathbf{k},\mathbf{R};i\Omega) = 2e^{-2|\Omega||\mathbf{R}\cdot\mathbf{e}_z|/\hbar v_{\uparrow z}} \times \begin{cases} r_{\rm eh}(\mathbf{k}_\parallel;i|\Omega|) & \text{if } k_z<0 \text{ and } \Omega>0, \\ -r_{\rm he}(\mathbf{k}_\parallel;i|\Omega|)^* & \text{if } k_z>0 \text{ and } \Omega<0, \\ 0 & \text{otherwise.} \end{cases} \tag{81}$$

The function f may be identified with the anomalous Green function in the quasiclassical theory.[48] Note that f is nonzero only if the wave vector $\mathbf{k}$ points away from the superconductor interface if $\Omega>0$ (corresponding to a hole moving toward the superconductor, retarded case), or if $\mathbf{k}$ points toward the superconductor if $\Omega<0$ (corresponding to an electron moving toward the superconductor, advanced case).

Because of the δ function in Eq. (80), the function f is meaningful for wave vectors $\mathbf{k}$ with $|\mathbf{k}|=k_\uparrow$ only. Following the literature, we analyze moments of f, taken with respect to its angular dependence on $\mathbf{k}$, and determine whether these are even or odd functions of the Matsubara frequency Ω. The moments are defined through the relation

$$f(\mathbf{k},\mathbf{R};i\Omega)=\sum_{l,m} Y_{lm}(\mathbf{e}_\mathbf{k}) f_{lm}(\mathbf{R};i\Omega), \tag{82}$$

where Y_{lm} is a spherical harmonic and $\mathbf{e}_\mathbf{k}=\mathbf{k}/k$ the unit vector in the direction $\mathbf{k}$. We restrict the discussion below to $l=0$ and $l=1$.

In order to determine the parity of the moments f_{lm}, we note that

$$r_{\rm eh}(\mathbf{k}_\parallel,i|\Omega|)=r_{\rm he}(-\mathbf{k}_\parallel,i|\Omega|)^*,$$

see Sec. II. If the magnetization gradient is perpendicular to the half-metal–superconductor interface, $r_{\rm he}(-\mathbf{k}_\parallel,i|\Omega|)$ is an odd function of frequency, proportional to Ω for small frequencies, but an even function of $\mathbf{k}_\parallel$, see Eq. (40). Hence f_{00} is an odd function of Ω, proportional to Ω for small frequencies.[36,46] The moment f_{10} is an even function of Ω, proportional to $|\Omega|$ for small Ω. The functions f_{1m} with $m=\pm1$ are both zero. If the magnetization gradient is parallel to the half-metal–superconductor interface, $r_{\rm he}(-\mathbf{k}_\parallel,i|\Omega|)$ is an even function of frequency, with a finite value for $\Omega\to0$, but an odd function of $\mathbf{k}_\parallel$, see Eq. (41). This implies that f_{00} and f_{10} are both zero, whereas f_{1m} with $m=\pm1$ are even functions of Ω, with a finite nonzero value in the limit $\Omega\to0$.

The moments f_{lm} calculated via the scattering approach obey the general symmetries imposed by the Pauli principle: For proximity effects induced by an s-wave, spin-singlet superconductor, the anomalous Green function $f_{lm}(i\Omega)$ in a half-metal is an odd function of Ω for even l and an even function of Ω for odd l.[27,46] Although $f_{00}(i\Omega)\to0$ for $\Omega\to0$ in the two cases discussed above, the requirement that the s-wave amplitude $f_{00}(i\Omega)$ be an odd function of Ω does not necessarily imply that $f_{00}(i\Omega)$ always vanishes in this limit. Indeed, in junctions between a superconductor and a standard (not half-metallic) ferromagnet, it is known that the triplet component of $f_{00}(i\Omega)$ approaches a finite value if $\Omega\to0$. [To be precise, the triplet component of $f_{00}(i\Omega)\propto\mathrm{sign}\,(i\Omega)$ for small Ω for a ferromagnet, in order to satisfy the antisymmetry constraint.[3,26,46]] For junctions involving a half-metal, an example of such a singular frequency dependence is given by the case of a lateral contact to a thin half-metallic film case, which we now discuss.

As in Sec. V, we consider the case that the magnetization direction does not depend on y, and that the region of nonuniform magnetization is limited to the vicinity of $x=0$. We assume that the inequalities described in the paragraph following Eq. (61) are obeyed, so that the thin-film reflection matrix $r_{\rm he}^{\rm eff}$ is diagonal in the transverse-mode indices n and n'. We calculate the anomalous Green function $F(\mathbf{r},\mathbf{r}';i\Omega)$ for the case that the coordinates $\mathbf{r}$ and $\mathbf{r}'$ are on the positive-x side of the region with nonuniform magnetization. Expanding the Green function in transverse modes, one then finds

$$F(\mathbf{r},\mathbf{r}';i\Omega) = \frac{1}{4\pi^2 i}\int d\mathbf{k}\sin(k_z z)\sin(k_z z')\, e^{i\mathbf{k}_\parallel\cdot(\mathbf{r}-\mathbf{r}')} \times f_n(\mathbf{k}_\parallel,\mathbf{R};i\Omega)\delta(\varepsilon_k-\mu_{\rm H\uparrow}), \tag{83}$$

where

$$f_n(\mathbf{k}_\parallel,\mathbf{R};i\Omega) = 2e^{-2|\Omega|(\mathbf{R}\cdot\mathbf{e}_x)/\hbar v_{\uparrow x}} \times \begin{cases} r_{\rm eh}^{\rm eff}(\mathbf{k}_\perp;i|\Omega|) & \text{if } k_x>0 \text{ and } \Omega>0, \\ -r_{\rm he}^{\rm eff}(\mathbf{k}_\perp;i|\Omega|)^* & \text{if } k_x<0 \text{ and } \Omega<0, \\ 0 & \text{otherwise.} \end{cases} \tag{84}$$

The moments f_{lm} with $m+l$ odd vanish in the thin film geometry because they are odd in k_z. Hence, we expand $f_n(\mathbf{k}_\parallel,\mathbf{R};i\Omega)$ in moments as

$$f_n(\mathbf{k}_\parallel,\mathbf{R};i\Omega)=\sum_{l+m\ \text{even}} Y_{lm}(\mathbf{e}_k) f_{lm}(\mathbf{R};i\Omega), \tag{85}$$

where $\mathbf{e}_\mathbf{k}$ is the unit vector pointing in the direction of $\mathbf{k}$. In the thin-film geometry, the lowest moment f_{00} is not only nonzero for magnetization gradients perpendicular to the surface, but also for magnetization gradients parallel to the surface. In both cases f_{00} is an odd function of the

frequency Ω, but f_{00} is discontinuous at $\Omega = 0$, $f_{00} \propto \mathrm{sign}(\Omega)$. [For the case of magnetization gradient perpendicular to the HS interface, the Ω dependence of $f_{00}(i\Omega)$ is modified for energies below the Thouless energy $\hbar v_\uparrow / W_x$ of the lateral contact.]

The fact that the s-wave amplitude $f_{00}(i\Omega)$ may have a finite limit in the limit $\Omega \to 0$ is a striking difference between the thin-film geometry and the regular geometry with a half-infinite half-metal. Thus, our calculation identifies geometry as an important second factor in determining the symmetries of the anomalous Green function—in addition to the Pauli principle.

VII. CONCLUSION

In this article we have calculated the Andreev reflection amplitudes of a half-metal–superconductor (HS) junction with a spatially nonuniform magnetization direction in the half-metal. General symmetry considerations enforce that the Andreev reflection amplitude r_{he} is zero at the Fermi level $\varepsilon = 0$, except if inversion symmetry around the normal to the HS interface is broken.[29,32] On the other hand, if that is the case, r_{he} is an odd function of the wave-vector component $\mathbf{k}_\parallel$ parallel to the interface. These general results were confirmed by explicit calculations of r_{he} for magnetization gradients parallel and perpendicular to the interface, and they were applied to calculations of the subgap conductance and the Josephson effect in impurity-free HS and SHS junctions. With one exception, the voltage and temperature dependences of the conductance and the Josephson current showed remarkable differences between the cases with and without inversion symmetry, where the precise form of these differences depends on the contact geometry. (The exception is the Josephson current in a lateral SHS junction, which shows little differences between the scenarios with and without inversion symmetry.)

Impurity scattering has not been included in the calculations presented here. As discussed in the Introduction, this is not a serious shortcoming for the microscopic Andreev reflection amplitude r_{eh} (the amplitude for a single reflection of a quasiparticle incident on the HS interface) if the disorder is weak (mean free path l much larger than the Fermi wavelengths in the superconductor or in the half-metal, and than the wave-function decay length in the half-metal), because Andreev reflection is a process that takes place on these microscopic length scales.[2] Hence, the microscopic reflection amplitudes r_{eh} of Sec. IV can be used as a valid starting point for a scattering theory of a disordered HS junction. The same situation occurs at normal-metal–superconductor (NS) interfaces, where the Andreev reflection amplitudes of a clean NS interface are combined with standard theoretical methods for disordered normal metals in order to construct a theory of a disordered NS junction.[42]

However, disorder has a profound effect on the type and magnitude of the induced superconducting correlations in the half-metal, which are mediated by the effect of multiple Andreev reflections. This includes the calculation of the effective Andreev reflection amplitude $r_{\mathrm{he}}^{\mathrm{eff}}$ in the thin-film geometry, which represents the coherent effect of multiple Andreev reflections. In the absence of disorder, the wave-vector component $\mathbf{k}_\parallel$ parallel to the HS interface is conserved, and multiple Andreev reflections at the HS interface always add constructively.[32] With disorder, $\mathbf{k}_\parallel$ is no longer conserved. Because the sign of the Andreev reflection amplitudes r_{eh} depends on the angle between $\mathbf{k}_\parallel$ and the gradient of the magnetization angle, interference between multiple reflection events need no longer be constructive. In particular, the p-wave superconducting correlations induced by a magnetization gradient parallel to the HS interface are strongly sensitive to disorder, and unable to survive for large distances away from the superconductor.[49] A detailed study of disorder effects in a lateral contact between a thin half-metallic film and a superconductor is left for a future publication.

We close by noting that very recently half-metal–superconductor hybrid systems have garnered attention as possible candidates for the creation of Majorana fermion excitations,[50] which are considered promising candidates to implement topological quantum computing.[51,52] While the system considered here is too elementary to be useful for quantum computation, the fundamental ingredients present here—spin-flip scattering, half-metallicity, and s-wave superconducting order—are precisely the same as those appearing in the proposals for Majorana fermion excitations.[50] Further analysis of common and distinguishing features is thus desirable.

ACKNOWLEDGMENTS

We gratefully acknowledge stimulating discussions with Benjamin Beri, Norman Birge, Mathias Duckheim, Francis Wilken, Dan Ralph, and Boris Spivak. This work was supported by the Cornell Center for Materials Research under NSF Grant No. 0520404 and by the Alexander von Humboldt Foundation.

APPENDIX: EXPLICIT CALCULATION OF THE GAUGE TRANSFORMATION

In this Appendix we consider a general variation the magnetization direction, described by variations of both polar angles θ_{m} and ϕ_{m}. If both θ_{m} and ϕ_{m} are position dependent, the transformation given in Eq. (35) leads to the gauge potential

$$\begin{aligned}\mathbf{A} = \frac{\hbar}{2}\,[&(\sigma_2 \cos\phi_{\mathrm{m}} - \sigma_1 \sin\phi_{\mathrm{m}})\nabla\theta_{\mathrm{m}} \\ &- (\sigma_1 \cos\phi_{\mathrm{m}} \sin\theta_{\mathrm{m}} + \sigma_2 \sin\phi_{\mathrm{m}} \sin\theta_{\mathrm{m}})\nabla\phi_{\mathrm{m}} \\ &- \sigma_3(1 - \cos\theta_{\mathrm{m}})\nabla\phi_{\mathrm{m}}]\,. \end{aligned} \tag{A1}$$

In the calculation of Sec. IV only the terms proportional to $\nabla\theta_{\mathrm{m}}$ were included. There are three terms proportional to $\nabla\phi_{\mathrm{m}}$. Of these, the term proportional to σ_3 does not contribute to spin-flip Andreev reflection. Repeating the calculation of Sec. IV with the two remaining terms proportional to $\nabla\phi_{\mathrm{m}}$ gives the results (40) and (41) for gradients perpendicular and parallel to the interface, respectively, with the replacement $\nabla\theta_{\mathrm{m}} \to \nabla\theta_{\mathrm{m}} + i \sin\theta_{\mathrm{m}} \nabla\phi_{\mathrm{m}}$. In the general case that the magnetization gradient has components parallel and perpendicular to the interface, the Andreev reflection amplitudes of Eqs. (40) and (41) must be added.

[1] Y. Imry, *Introduction to Mesoscopic Physics* (Oxford University Press, Oxford, 2002).
[2] A. F. Andreev, Zh. Eksp. Teor. Fiz. **46**, 1823 (1964) [Sov. Phys. JETP **19**, 1228 (1964)].
[3] F. S. Bergeret, A. F. Volkov, and K. B. Efetov, Phys. Rev. Lett. **86**, 4096 (2001).
[4] F. S. Bergeret, A. F. Volkov, and K. B. Efetov, Phys. Rev. B **64**, 134506 (2001).
[5] A. Kadigrobov, R. Shekhter, and M. Jonson, Europhys. Lett. **54**, 394 (2001).
[6] F. S. Bergeret, A. F. Volkov, and K. B. Efetov, Rev. Mod. Phys. **77**, 1321 (2005).
[7] I. Sosnin, H. Cho, V. T. Petrashov, and A. F. Volkov, Phys. Rev. Lett. **96**, 157002 (2006).
[8] V. N. Krivoruchko and V. Y. Tarenkov, Phys. Rev. B **75**, 214508 (2007).
[9] K. A. Yates, W. R. Branford, F. Magnus, Y. Miyoshi, B. Morris, L. F. Cohen, P. M. Sousa, O. Conde, and A. J. Silvestre, Appl. Phys. Lett. **91**, 172504 (2007).
[10] T. S. Khaire, M. A. Khasawneh, W. P. Pratt, and N. O. Birge, Phys. Rev. Lett. **104**, 137002 (2010).
[11] A. F. Volkov and K. B. Efetov, Phys. Rev. B **78**, 024519 (2008).
[12] A. F. Volkov, Y. V. Fominov, and K. B. Efetov, Phys. Rev. B **72**, 184504 (2005).
[13] Y. V. Fominov, A. F. Volkov, and K. B. Efetov, Phys. Rev. B **75**, 104509 (2007).
[14] J. Linder, T. Yokoyama, and A. Sudbø, Phys. Rev. B **79**, 054523 (2009).
[15] A. F. Volkov, A. Anishchanka, and K. B. Efetov, Phys. Rev. B **73**, 104412 (2006).
[16] G. B. Halász, J. W. A. Robinson, J. F. Annett, and M. G. Blamire, Phys. Rev. B **79**, 224505 (2009).
[17] M. Alidoust, J. Linder, G. Rashedi, T. Yokoyama, and A. Sudbø, Phys. Rev. B **81**, 014512 (2010).
[18] A. F. Volkov, F. S. Bergeret, and K. B. Efetov, Phys. Rev. Lett. **90**, 117006 (2003).
[19] M. Houzet and A. I. Buzdin, Phys. Rev. B **76**, 060504 (2007).
[20] V. Braude and Y. V. Nazarov, Phys. Rev. Lett. **98**, 077003 (2007).
[21] A. F. Volkov and K. B. Efetov, Phys. Rev. B **81**, 144522 (2010).
[22] L. Trifunovic and Z. Radović, Phys. Rev. B **82**, 020505 (2010).
[23] M. Houzet, Phys. Rev. Lett. **101**, 057009 (2008).
[24] M. Eschrig, J. Kopu, J. C. Cuevas, and G. Schön, Phys. Rev. Lett. **90**, 137003 (2003).
[25] Y. Asano, Y. Tanaka, and A. A. Golubov, Phys. Rev. Lett. **98**, 107002 (2007).
[26] Y. Asano, Y. Sawa, Y. Tanaka, and A. A. Golubov, Phys. Rev. B **76**, 224525 (2007).
[27] M. Eschrig and T. Löfwander, Nature Phys. **4**, 138 (2008).
[28] A. V. Galaktionov, M. S. Kalenkov, and A. D. Zaikin, Phys. Rev. B **77**, 094520 (2008).
[29] B. Béri, J. N. Kupferschmidt, C. W. J. Beenakker, and P. W. Brouwer, Phys. Rev. B **79**, 024517 (2009).
[30] R. S. Keizer, S. T. B. Goennenwein, T. M. Klapwijk, G. Miao, G. Xiao, and A. Gupta, Nature (London) **439**, 825 (2006).
[31] M. S. Anwar, F. Czeschka, M. Hesselberth, M. Porcu, and J. Aarts, Phys. Rev. B **82**, 100501(R) (2010).
[32] J. N. Kupferschmidt and P. W. Brouwer, Phys. Rev. B **80**, 214537 (2009).
[33] J. Linder, M. Cuoco, and A. Sudbø, Phys. Rev. B **81**, 174526 (2010).
[34] M. Duckheim and P. W. Brouwer, e-print arXiv:1011.5839.
[35] F. Wilken, diploma thesis, FU Berlin, 2010.
[36] M. Eschrig, Phys. Rev. B **80**, 134511 (2009).
[37] B. Béri, Phys. Rev. B **79**, 245315 (2009).
[38] M. S. Kalenkov, A. V. Galaktionov, and A. D. Zaikin, Phys. Rev. B **79**, 014521 (2009).
[39] G. E. Blonder, M. Tinkham, and T. M. Klapwijk, Phys. Rev. B **25**, 4515 (1982).
[40] C. W. J. Beenakker, Phys. Rev. Lett. **67**, 3836 (1991).
[41] P. W. Brouwer and C. W. J. Beenakker, Chaos Solitions Fractals **8**, 1249 (1997), see also e-print arXiv:cond-mat/9611162v3.
[42] C. W. J. Beenakker, in *Mesoscopic Quantum Physics*, edited by E. Akkermans, G. Montambaux, J.-L. Pichard, and J. Zinn-Justin (North-Holland, Amsterdam, 1995), p. 279.
[43] K. K. Likharev, Rev. Mod. Phys. **51**, 101 (1979).
[44] G. Miao, G. Xiao, and A. Gupta, Phys. Rev. B **71**, 094418 (2005).
[45] G. E. Volovik, J. Phys. C **20**, L83 (1987).
[46] M. Eschrig, T. Löfwander, T. Champel, J. C. Cuevas, J. Kopu, and G. Schön, J. Low Temp. Phys. **147**, 457 (2007).
[47] R. C. O'Handley, *Modern Magnetic Materials* (Wiley, New York, 2000).
[48] J. Rammer and H. Smith, Rev. Mod. Phys. **58**, 323 (1986).
[49] For an HS. junction with unconventional (d-wave) superconductor, a magnetization gradient parallel to the interface may lead to a spin-flip Andreev reflection amplitude $r_{\rm eh}$ that is no longer odd in $\mathbf{k}_\parallel$. In this case the induced superconducting correlations are not destroyed by disorder, see A. F. Volkov and K. B. Efetov, Phys. Rev. Lett. **102**, 077002 (2009).
[50] J. D. Sau, R. M. Lutchyn, S. Tewari, and S. Das Sarma, Phys. Rev. Lett. **104**, 040502 (2010).
[51] S. Das Sarma, M. Freedman, and C. Nayak, Phys. Rev. Lett. **94**, 166802 (2005).
[52] C. Nayak, S. H. Simon, A. Stern, M. Freedman, and S. Das Sarma, Rev. Mod. Phys. **80**, 1083 (2008).